

# Two-stage stochastic programming models for the extended aircraft arrival management problem with multiple pre-scheduling points

Ahmed Khassiba <sup>a,\*</sup>, Sonia Cafieri <sup>a</sup>, Fabian Bastin <sup>b</sup>, Marcel Mongeau <sup>a</sup>,  
Bernard Gendron <sup>b</sup>

<sup>a</sup> Ecole Nationale de l'Aviation Civile, Université de Toulouse, France

<sup>b</sup> Université de Montréal, DIRO, CIRRELT, QC, Canada

## Keywords:

Extended aircraft arrival management

Two-stage stochastic programming

Uncertainty

---

Extended aircraft arrival management under uncertainty has been previously studied in the literature using two-stage stochastic optimization in the case of a single initial approach fix (IAF) and a single runway. In this paper, we propose an extension taking into account: (i) multiple IAFs feeding the landing runway, (ii) aircraft having different initial flight status (at-departure-gate or airborne) when making first-stage decisions, and (iii) a time-deviation cost function to minimize that is based on reference values depending on aircraft type and flight phase. Two problem variants are modeled according to the degree of freedom on IAF assignment to aircraft. In the first variant, IAFs are to be assigned to aircraft, as a first-stage decision. In the second variant, IAF assignment is fixed and considered as a problem input. Numerical results on realistic instances from Paris Charles-de-Gaulle airport confirm the benefit of taking into account uncertainty through two-stage stochastic programming, and through re-assignment of IAFs.

## 1. Introduction

AMAN (for *Arrival MANager*) is a crucial decision-support system for European air traffic controllers (ATCOs) to sequence and schedule, safely and efficiently, aircraft arrivals on busy airports (Hasevoets and Conroy, 2010). AMAN's current operational horizon is around 100–200 nautical miles (NM) from the destination airport, *i.e.*, 30–45 min before landing. In the near future, AMAN is foreseen to be upgraded in order to capture aircraft at a distance up to 500 NM, *i.e.*, 2–3 h before landing (Tielrooij et al., 2015). Extending AMAN's horizon is expected to allow ATCOs to start sequencing and scheduling earlier, when aircraft are still in their cruise phase or at their departure gate, which promotes more eco-efficient aircraft trajectories and hopefully improves airport capacity and reduces delays. However, at this extended horizon, uncertainty is significant when predicting landing times and expected times to start the *approach phase* (which corresponds to the flight phase where aircraft are around 40 NM far from the landing runway, at an altitude of 3000 ft, and getting ready for landing).

The classical problem of sequencing and scheduling aircraft landings in a relatively short operational horizon has been widely studied in the literature, from the 1970's (Dear, 1976; Psaraftis, 1978). Most of the literature focuses on the deterministic case, where all data is assumed to be known with certainty (Balakrishnan and Chandran, 2010; Beasley et al., 2000). For recent surveys, the reader is redirected to Bennell et al. (2011), Ikli et al. (2021). A recent review on stochastic modeling applications in air traffic

---

\* Corresponding author.

E-mail address: [ahmed.khassiba@enac.fr](mailto:ahmed.khassiba@enac.fr) (A. Khassiba).

<sup>1</sup> Research & Development Engineer, Ph.D.

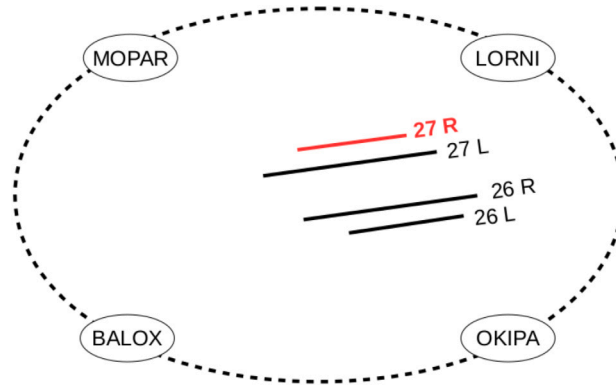


Fig. 1. Simplified scheme of IAFs surrounding CDG's runways (not to scale).

management can be found in [Shone et al. \(2021\)](#). Different optimization paradigms, such as two-stage stochastic programming ([Birge and Louveaux, 2011](#)), have been successfully applied to air traffic flow management problems ([Corolli et al., 2015](#)), and specifically to the aircraft scheduling problem, under uncertain arrival times, with short operational horizon ([Liu et al., 2018](#); [Sölveling and Clarke, 2014](#); [Sölveling et al., 2011](#)). Extensions to various types of disturbances and uncertainties have also been addressed in a number of papers related to aircraft scheduling in the terminal manoeuvring area (TMA) ([Huo et al., 2021](#); [Samà et al., 2014](#); [Scala et al., 2021](#)).

The problem of extended aircraft arrival management under uncertainty has been introduced by [Khassiba et al. \(2019\)](#) as the optimization problem consisting in pre-scheduling aircraft arrivals, 2–3 h before their planned landing times, on a reference air-traffic route point in the terminal area, called the initial approach fix (IAF), so as to prepare for more efficient inbound air traffic handling, through the terminal area up until landing. The operational setup in [Khassiba et al. \(2019\)](#) involves a set of aircraft arrivals, planning to fly over the same IAF and to land on the same runway. In [Khassiba et al. \(2020\)](#), the authors formulate this problem using a two-stage stochastic mixed-integer programming model with chance constraints. Their first-stage optimization problem determines target times over the IAF together with the target sequence in which aircraft should arrive at the IAF, that they refer to as the *target IAF sequence*. Their first-stage objective is to minimize the “landing sequence length”, expressed as the sum of *final-approach separations* between all pairs of successive aircraft in the landing sequence. Since, for each pair, the final approach separation depends on the aircraft *wake-turbulence categories*, different landing sequences yield different utilization times of the runway. For that reason, minimizing the landing sequence length is used in [Khassiba et al. \(2020\)](#) as a surrogate for maximizing the runway throughput. While *target* IAF times are determined in the first stage (together with the *target* IAF sequence), *actual* times over the IAF are assumed to deviate randomly from these target times following known probability distributions. In the second stage, actual IAF times are assumed to be revealed, hence landing times are determined in view of minimizing a time-deviation cost function. Remark that the *target* landing sequence is assumed to be the same as the target IAF sequence. Compared to their deterministic counterparts, the stochastic solutions obtained in [Khassiba et al. \(2019, 2020\)](#) are shown to be more robust to the uncertainty occurring within the 2–3 h before landing.

In this paper, we propose an extension of the two-stage stochastic optimization approach of [Khassiba et al. \(2020\)](#) to a more realistic operational context. First, we consider that there are multiple IAFs feeding the same runway. Second, additionally to wake-turbulence categories, we take into account the aircraft types and the flight status (e.g., still at departure gate or already airborne) when making first-stage decisions. Third, we optimize a single criterion: the total delay cost, based on delay-cost reference values, detailed by aircraft type and flight phase, reported in the literature. The following remarks motivate these choices. First, in major airports, there are usually several IAFs that feed the landing runway(s). For example, in Paris Charles-de-Gaulle airport (CDG), the northern landing runway 27R is mainly fed by two IAFs, named MOPAR and LORNI, while the southern landing runway 26L is usually fed by two other IAFs, named OKIPA and BALOX (see [Fig. 1](#)). Second, the integration of several aircraft features when making first-stage decisions, is likely to lead to a finer definition of the problem and to a better assessment of the arrival schedule quality. For example, an aircraft that is still at the departure gate when making first-stage decisions can be delayed on ground. In terms of fuel consumption, ground delay with engines turned off is much more efficient than delay during en-route and approach phases. Hence, flights that have not taken off yet, at the moment of making first-stage decisions, have a cost-efficient delay option that airborne flights do not have. Third, in the widely-used delay-cost reference-values report ([Cook and Tanner, 2015](#)), the delay cost is reported as a function of the length of the delay for fifteen commercial aircraft types and four flight phases. Using these reference values, piecewise-linear convex increasing delay cost functions can be obtained. This opens the opportunity to optimize a single consistent criterion, the total delay cost, that takes into account several realistic features of the considered flights. Also, the interpretation of the objective function value and of the value of the stochastic solution is more straightforward than for the studied criteria in [Khassiba et al. \(2019, 2020\)](#).

We address the above-mentioned points as follows. As regards IAFs, we consider several IAFs feeding a single landing runway. Usually, IAFs are pre-assigned to aircraft arrivals according to their geographical origin and to their aircraft propulsion type (e.g.,

see Meyn and Erzberger (2005, Figure 1)). Hence, in our study, we assume that every flight is planned to fly over a given IAF, known in advance, referred to as the *initial IAF*. From an operational viewpoint, changing the IAF of a flight usually follows a change of landing runway for this flight, since each runway is fed by a specific subset of IAFs. For instance, consider an aircraft arriving at CDG from the north-west, planning to land on runway 27R, and to cross IAF MOPAR beforehand. If this aircraft is re-scheduled to land on the southern runway 26L (regardless the operational reason), then its IAF is likely to be updated to the south-western IAF, BALOX. An aircraft can also be asked to change its IAF in case of adverse weather affecting approach procedures from its initial IAF. Finally, an aircraft can be assigned to a different IAF in order to distribute better aircraft arrival flows and to avoid holding delays. Such an operational procedure is called *fix balancing* (Kistan et al., 2017). In this study, we propose two problem variants corresponding to this multi-IAF setup. In the first variant, the decision maker has to assign an IAF to each aircraft in the first stage, possibly different from its initial IAF. In the second variant, IAF assignment is considered as an input, i.e., each aircraft must fly over its initial IAF. The second-stage problem is the same for both variants, and seeks to schedule aircraft, assumed to be close to the considered IAFs, in order to land on the (unique) runway. Moreover, we consider that at the time of the first-stage decisions (typically 2-3 h before planned landing), each aircraft can be in one of the two status: either *on-ground* or *airborne*. On-ground aircraft are at their departure gate with engines turned off. Airborne aircraft have already taken off, and are assumed to be in their cruise phase at the time of first-stage decisions. In the first stage, on-ground and airborne aircraft are to be given target IAF times, as in Khassiba et al. (2019, 2020). In this paper, an additional first-stage decision is to be made for each on-ground aircraft: determining a target take-off time. We assume that target take-off times can be met with certainty. Our objective function is the expectation of the total time-deviation cost, to be minimized, where the time-deviation cost depends on both the aircraft type (A320, B763, etc.) and the flight phase (at-departure-gate, en-route, or approach). Reference values of delay and advance cost, for each aircraft type at each flight phase, are based on Cook and Tanner (2015).

The remainder of the paper is organized as follows. In Section 2, the problem statement is given. Section 3 presents the two-stage stochastic programming model of the first variant (IAF assignment as a first-stage decision). Section 4 derives the mathematical model of the second variant (IAF assignment as a problem input). A preliminary computational study is reported in Section 6. Concluding remarks and perspectives are given in Section 7.

## 2. Problem statement

We consider  $n$  aircraft planning to land on the same runway, while there are  $m < n$  available IAFs over which any aircraft can fly before landing. Initially, each aircraft is assigned to one IAF, called its *initial IAF*, and assumed to be the IAF closest to each aircraft's planned route. We assume that these aircraft are considered at the same instant, 2-3 h before their planned landing times. At this time horizon, the considered aircraft are partitioned into two subsets, depending on their flight status. There are  $n_G$  aircraft that are still in their departure gate with engines turned off, called *on-ground* aircraft; and  $n_A$  aircraft that have already taken off, called *airborne* aircraft, and assumed to be in their cruise phase. We seek to schedule the  $n$  aircraft on the  $m$  available IAFs, so as to optimize the *expectation* of the delay-cost function, assuming that actual arrival times to IAFs cannot be predicted with certainty. In this context, scheduling consists of the following decisions. Each aircraft has to be assigned to exactly one IAF (possibly different from its initial IAF, for the more general problem variant) while all aircraft will land on the same (unique) runway. For each on-ground aircraft, a *target take-off time* is to be determined. Pilots and air traffic controllers are assumed to be able to meet these target times with high accuracy. In other words, we consider that target take-off times are not affected by uncertainty. Moreover, for each aircraft, regardless its flight status, a *target IAF time* is to be computed. Finally, the order in which aircraft should arrive to their assigned IAF, forming what we shall call *target IAF sequences*, has to be determined, as well as a *target landing sequence*. An operational setup with  $m = 2$  IAFs and a single landing runway is illustrated in Fig. 2.

Let  $\mathcal{A} = \{1, 2, \dots, n\}$  denote the set of aircraft indices. Let  $\mathcal{A}^G$ , the set of on-ground aircraft indices, and  $\mathcal{A}^A$ , the set of airborne aircraft indices, be such that:

$$\mathcal{A} = \mathcal{A}^G \cup \mathcal{A}^A \quad \text{and} \quad \mathcal{A}^G \cap \mathcal{A}^A = \emptyset \tag{1}$$

Let  $\mathcal{I} = \{1, 2, \dots, m\}$  denote the set of IAF indices. Each aircraft  $a \in \mathcal{A}$  has a *planned landing time*  $P_a^L$  known in advance, where “L” stands for landing. Let  $i_a^* \in \mathcal{I}$  denote the index of the initial IAF for aircraft  $a \in \mathcal{A}$ . To simplify the notation, and as long as there is no ambiguity, we shall drop the aircraft subscript  $a$  from the IAF index, keeping solely the star superscript (\*) to refer to the initial IAF for the considered aircraft. For each IAF  $i \in \mathcal{I}$  and each aircraft  $a \in \mathcal{A}$ , we are provided with an *unimpeded flight time*  $\hat{V}_a^i$ : it is the time required for aircraft  $a$  to fly from IAF  $i$  to touch down on the landing runway, as if it were alone in the terminal area. In the following, we present the input data notation for each aircraft according to its flight status: airborne or on-ground.

*Airborne aircraft.* For each airborne aircraft  $a \in \mathcal{A}^A$ , we can compute a *planned IAF time at its initial IAF*  $i^* \in \mathcal{I}$ , denoted  $P_a^{i^*}$ , through direct reverse planning as follows:

$$P_a^{i^*} = P_a^L - \hat{V}_a^{i^*} \tag{2}$$

Since the initial IAF for a given aircraft is assumed to be the IAF closest to its planned route, deciding to reroute an aircraft  $a \in \mathcal{A}^A$  from its initial IAF  $i^* \in \mathcal{I}$  to a different IAF  $j \in \mathcal{I} \setminus \{i^*\}$  incur a positive rerouting delay noted  $r^{i^*j} > 0$ . We set  $r^{ii} = 0$ . Hence, for an aircraft  $a \in \mathcal{A}^A$ , the *planned IAF time at any IAF*  $j \in \mathcal{I}$ , denoted  $P_a^j$ , can be expressed as:

$$P_a^j = P_a^{i^*} + r^{i^*j} \tag{3}$$

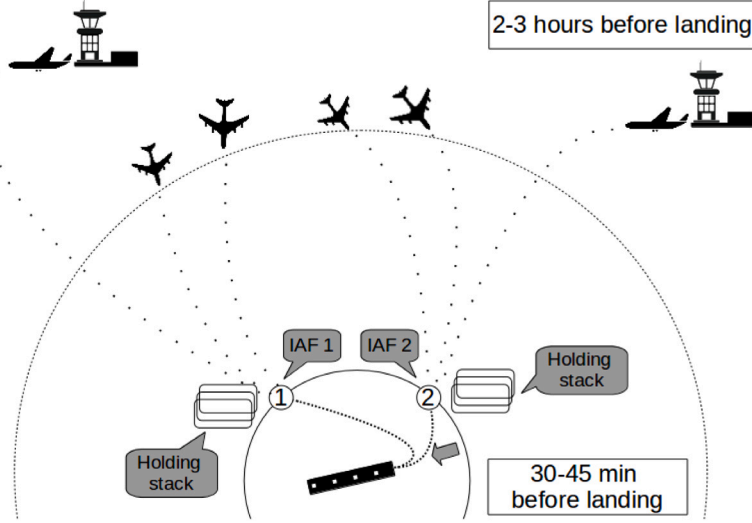


Fig. 2. Operational environment with two IAFs (not to scale).

*On-ground aircraft.* For each on-ground aircraft  $a \in \mathcal{A}^G$ , we are provided with a planned take-off time,  $P_a^{\text{TOT}}$ , and an unimpeded flight time from the origin airport of  $a$  to its initial IAF  $i^* \in \mathcal{I}$ , that we denote  $\hat{V}_a^O$ . While an aircraft is still at its departure gate, its take-off time can be delayed up to a given amount of time, denoted  $\bar{d}_a^G > 0$ . The *target take-off time* for an on-ground aircraft  $a \in \mathcal{A}^G$  must lie within the time window  $[P_a^{\text{TOT}}, P_a^{\text{TOT}} + \bar{d}_a^G]$ . In practice, a departure slot (or Calculated Take-Off Time — CTOT) is defined as an interval including the departure time and a tolerance of 15-minute length. We assume that the target take-off time in this study can be chosen within an interval of a similar length. For the sake of simplification, we assume that there are no local (origin airport) constraints on the departure time of on-ground aircraft.

Note that, as soon as the target take-off time of an on-ground aircraft  $a \in \mathcal{A}^G$  is decided, we can compute the *unconstrained IAF time*,  $U_a^{O \rightarrow i^*}$ , at which  $a$  would reach its initial IAF  $i^* \in \mathcal{I}$ , as the sum of the target take-off time, and  $\hat{V}_a^O$  the unimpeded flight time from the origin airport to the initial IAF. The unconstrained time at which  $a$  reaches any other IAF  $j \in \mathcal{I} \setminus \{i^*\}$ , denoted  $U_a^{O \rightarrow j}$ , is obtained by adding the rerouting delay,  $r^{i^*j} > 0$ , to  $U_a^{O \rightarrow i^*}$ .

During the en-route flight phase, with 2–3 h look-ahead time, it is possible to expedite or delay an aircraft  $a \in \mathcal{A}$  by a given amount of time, mainly through speed change. Let us denote  $\underline{d}_a^R$  and  $\bar{d}_a^R$ , respectively, the *maximal possible time saving*, and the *maximal possible delay* for aircraft  $a$  during its en-route phase. This allows us to compute an *earliest*, and a *latest IAF time* at each IAF  $i \in \mathcal{I}$  (either its initial IAF, or any other one), denoted  $E_a^i$ , and  $L_a^i$  respectively, as follows:

$$E_a^i = P_a^i - \underline{d}_a^R \quad (4)$$

$$L_a^i = P_a^i + \bar{d}_a^R \quad (5)$$

Note that for an airborne aircraft  $a \in \mathcal{A}^A$ , the values of  $E_a^i$  and  $L_a^i$  are computed directly from known input data, while for an on-ground aircraft  $a' \in \mathcal{A}^G$ ,  $E_{a'}^i$  and  $L_{a'}^i$  depend on the decision variable: the target take-off time.

For an aircraft  $a \in \mathcal{A}$  and its assigned IAF  $i \in \mathcal{I}$ , let  $[E_a^i, L_a^i]$  denote the IAF time window, in which the *target IAF time* for  $a$  must lie (regardless its initial flight status). Hence, each aircraft has  $m$  IAF time windows, one for each possible IAF. After assigning each aircraft to one IAF, a *target IAF sequence* is to be found for each IAF. For any pair of successive aircraft assigned to the same IAF, a minimal distance separation must be satisfied. In practice, this IAF distance separation is independent of the aircraft pair and is identical for all IAFs. For modeling and optimization purposes, we convert this minimal distance separation into a minimal time separation, that we denote  $\underline{S}$ . Assuming a typical aircraft speed of 250 kts, and a minimal distance separation at IAF of 5 NM,  $\underline{S}$  can be set to 72 s (Khassiba et al., 2019). Finally, a *target landing sequence* is to be found as the merging of the different target IAF sequences.

When flying from 2–3 h to 30–45 min before landing, aircraft are subject to unpredicted phenomena (e.g., bad weather, en-route control actions, etc) affecting their ability to reach their IAF at the prescribed target time, with high accuracy. We assume that their *actual IAF times* deviate from their target times by random amounts of time (advance or delay) according to known probability distributions. In a realistic setting, uncertainty on IAF times decreases continuously over time, as aircraft get closer to IAFs. Consider an “early” aircraft very close to the terminal area, and assume that its actual IAF time is known (or, at least, can be predicted) with certainty. At the same time, other aircraft can still be very far from IAFs, and their actual times are still highly uncertain. However, such far aircraft do not have any impact on the scheduling of the “early” aircraft. In the current problem statement, we disregard such situations by assuming a set of aircraft in the first stage having their IAF times relatively close to each other. Hence, when the “earliest” aircraft becomes very close to its IAF, the “latest” aircraft is less than 30-min far from its IAF.

**Table 1**

Final-approach separations (in seconds) according to wake-turbulence categories from the International Civil Aviation Organization (ICAO) (Frankovich, 2012).

		Following aircraft		
		H	M	L
Leading aircraft	H	96	157	207
	M	60	69	123
	L	60	69	82

When all considered aircraft are within this short time horizon (corresponding to 30–45 min from landing), ground-based trajectory prediction from AMAN is assumed very accurate, and all actual IAF times can be assumed to be known with certainty. In this short time horizon corresponding to AMAN’s operational horizon, approach ATCOs have to schedule aircraft from the  $m$  different IAFs to land on the same runway. This corresponds to a second decision stage where a *target landing time* is to be determined for each aircraft, while the target landing sequence has already been determined at the larger time horizon of 2–3 h.

In the case of congestion in the terminal area, ATCOs may resort to *holding stacks* near IAFs, in order to further delay some aircraft, before landing. Holding stacks are air-route deviation structures allowing controllers to delay aircraft by keeping them flying circularly in confined areas, usually neighboring IAFs. However, the delay that can be absorbed by holding stacks and other control techniques (such as path stretching) in the terminal area is bounded above by a given amount of time, noted  $\hat{d}_a^T$  for aircraft  $a \in \mathcal{A}$ . Also, there is room for expediting an aircraft  $a \in \mathcal{A}$  (e.g., through path shortening) within the terminal area, which may save some amount of time, not exceeding a given limit, denoted  $\underline{d}_a^T$ , with respect to the unimpeded flight time,  $\hat{V}_a^i$ . Given these maximal possible time saving and delay in the terminal area, a *minimal* and a *maximal flight times*, denoted  $\underline{V}_a^i$  and  $\overline{V}_a^i$  respectively, can be defined for every aircraft  $a \in \mathcal{A}$  and every IAF  $i \in \mathcal{I}$ , as follows:

$$\underline{V}_a^i = \hat{V}_a^i - \underline{d}_a^T \quad (6)$$

$$\overline{V}_a^i = \hat{V}_a^i + \hat{d}_a^T \quad (7)$$

Moreover, for any pair of aircraft landing successively, a minimal distance separation must be satisfied during the final-approach phase. Final-approach separations depend on the wake-turbulence categories of the pair of considered aircraft, as defined by the International Civil Aviation Organization (ICAO): Heavy (H), Medium (M), and Light (L). For modeling and optimization purposes, we convert these minimal distance separations into *minimal time separations* (see Table 1 for numerical values), that we denote  $S_{ab}$ , for an ordered pair of aircraft  $(a, b) \in \mathcal{A} \times \mathcal{A}$ , such that  $a \neq b$ .

In the following, we formulate the extended aircraft arrival management problem with multiple IAFs, using the framework of two-stage stochastic programming. The first-stage time frame starts from 2–3 h before landing, when on-ground aircraft are to be scheduled for take-off and all aircraft are to be scheduled on the available IAFs. The second-stage time frame starts from 30–45 min before landing, when all aircraft are close to their IAF. The objective function to minimize is the total time-deviation cost over all aircraft and through the different flight phases. Reference values of delay cost in air transportation are specified in Cook and Tanner (2015), by aircraft type and flight phase. Advance cost can be estimated based on observations in Lee (2008). Our problem statement covers three flight phases for on-ground aircraft (at-departure-gate, en-route, and approach) and two flight phases for airborne aircraft (en-route and approach). The at-departure-gate delay involves no uncertainty, since on-ground aircraft are assumed to take off exactly at their target times. Hence, at-departure-gate delay cost is to be minimized in the first stage. For en-route and approach delay costs, they are to be minimized in the second stage, since they depend on the random actual IAF times.

We derive two variants from the extended aircraft arrival management problem with multiple IAFs, introduced above. Both variants follow the same two-stage partition, but they differ in terms of first-stage decisions. The first variant includes IAF assignment to aircraft as an additional first-stage decision, while in the second variant, IAF assignment is given and fixed: each aircraft will head to its initial IAF. The two-stage stochastic programming model of each variant is detailed in the next two sections.

### 3. First-variant model: IAF assignment as a (first-stage) decision

The general statement of the problem of extended aircraft arrival management problem with multiple IAFs, presented in Section 2, assumes that although each aircraft has an initial IAF, any aircraft can still be rerouted to a different IAF. We propose to formulate this general case, under uncertainty on IAF times, with a two-stage stochastic programming model, inspired by the model proposed in Khassiba et al. (2020). All notations are summarized in Table 2. The main components of the mathematical model of each stage (decision variables, operational constraints, and objective function) are described in the next two subsections. The full two-stage stochastic programming model is summarized in Section 3.3.

#### 3.1. First-stage problem

In the first stage, we determine a target take-off time for each on-ground aircraft  $a \in \mathcal{A}^G$ . We assign each aircraft  $a \in \mathcal{A}$  (on-ground or airborne) to one IAF  $i \in \mathcal{I}$ , and we determine a *target IAF time* for each aircraft. Also, we find a *target sequence on each IAF*. We assume that the *target landing sequence* is also determined in the first stage, and must be coherent with the merging

**Table 2**  
Notation summary.

Notation	Description
Sets:	
$\mathcal{A}$	Index set of aircraft
$\mathcal{A}^G$	Index set of on-ground aircraft
$\mathcal{A}^A$	Index set of airborne aircraft
$\mathcal{I}$	Index set of IAFs
$\mathcal{A}^{i^*}$	Index set of aircraft whose initial IAF is $i^* \in \mathcal{I}$
$\mathcal{A}^{i^*,G}$	Index set of on-ground aircraft whose initial IAF is $i^* \in \mathcal{I}$
$\mathcal{A}^{i^*,A}$	Index set of airborne aircraft whose initial IAF is $i^* \in \mathcal{I}$
Parameters:	
$P_a^L$	Planned landing time of aircraft $a \in \mathcal{A}$
$P_a^{i^*}$	Planned IAF time of aircraft $a \in \mathcal{A}^A$ at its initial IAF $i^*$
$P_a^j$	Planned IAF time of aircraft $a$ at an IAF $j$
$P_a^{\text{TOT}}$	Planned take-off time of aircraft $a \in \mathcal{A}^G$
$U_a^{O \rightarrow i^*}$	Unconstrained IAF time at which $a \in \mathcal{A}^G$ would reach its initial IAF $i^*$
$U_a^{O \rightarrow j}$	Unconstrained IAF time at which $a \in \mathcal{A}^G$ would reach IAF $j$
$E_a^i$	Earliest time for aircraft $a$ to reach IAF $i$
$L_a^i$	Latest time for aircraft $a$ to reach IAF $i$
$\rho^{ij}$	Delay due to rerouting from IAF $i$ to IAF $j$
$\hat{V}_a^O$	Unimpeded flight time from the origin airport of aircraft $a \in \mathcal{A}^G$
$\hat{V}_a^i$	Unimpeded time for aircraft $a$ to fly from IAF $i$ to the landing runway to its initial IAF $i^*$
$\underline{V}_a^i$	Minimal time for aircraft $a$ to fly from IAF $i$ to the landing runway
$\overline{V}_a^i$	Maximal time for aircraft $a$ to fly from IAF $i$ to the landing runway
$\underline{d}^G$	Maximum delay on-ground
$\overline{d}_a^R$	Maximal possible time saving for aircraft $a$ during en-route phase
$\underline{d}_a^R$	Maximal possible delay for aircraft $a$ during en-route phase
$\overline{d}_a^T$	Maximal possible time saving for aircraft $a$ during approach phase
$\underline{d}_a^T$	Maximal possible delay for aircraft $a$ during approach phase
$\underline{S}$	Minimal time separation between two consecutive aircraft at IAF
$S_{ab}$	Minimal final-approach time separation between leading aircraft $a$ and following aircraft $b$
$\omega_a$	Random variable of IAF time deviation of aircraft $a$
$\omega_a$	Realization of the random variable, IAF time deviation of aircraft $a$
$M_{ab}$	big-M constant enabling/disabling the separation constraint at IAFs between aircraft $a$ and $b$
$M_{ab}^L$	big-M constant enabling/disabling the separation constraint at the runway between aircraft $a$ and $b$
Cost functions:	
$f_a^G$	Cost function of the time deviation at gate of aircraft $a \in \mathcal{A}^G$
$f_a^R$	Cost function of the time deviation en route of aircraft $a$
$f_a^T$	Cost function of the time deviation in approach of aircraft $a$
Decision variables:	
• First stage:	
$x_a$	Target IAF time of aircraft $a \in \mathcal{A}$
$t_a$	Target take-off time of aircraft $a \in \mathcal{A}^G$
$\delta_{ab}$	Sequencing variable of aircraft pair $(a, b) \in \mathcal{A} \times \mathcal{A}$
$\zeta_{a,i}$	Assignment variable of aircraft $a$ to IAF $i$
$\phi_{ab}$	Binary variable of aircraft pair $(a, b) \in \mathcal{A} \times \mathcal{A}$ , equals 1 when both aircraft are assigned to the same IAF
• Second stage:	
$y_a$	Target landing time of aircraft $a \in \mathcal{A}$

of target sequences from all IAFs. In other words, aircraft assigned to the same IAF are not allowed to overtake each other while flying from the IAF to the runway. For instance, two aircraft  $a$  and  $b$  scheduled to cross the IAF  $i$  successively, such that  $a$  is before

$b$ , must land in the same relative order. However, a third aircraft  $c$  scheduled to cross IAF  $j \neq i$  can land in any position relatively to  $a$  and  $b$  (i.e.,  $c$  can land before  $a$  and  $b$ , or between  $a$  and  $b$ , or after  $a$  and  $b$ ).

Let  $\zeta_{ai}$  be a binary decision variable that assigns aircraft  $a \in \mathcal{A}$  to IAF  $i \in \mathcal{I}$ :

$$\zeta_{ai} = \begin{cases} 1 & \text{if aircraft } a \text{ is assigned to IAF } i \\ 0 & \text{otherwise} \end{cases}$$

To determine the target landing sequence of aircraft, we introduce a binary decision variable  $\delta_{ab}$  for each ordered pair of aircraft  $(a, b) \in \mathcal{A} \times \mathcal{A}$ ,  $a \neq b$ :

$$\delta_{ab} = \begin{cases} 1 & \text{if aircraft } a \text{ lands before aircraft } b \\ 0 & \text{otherwise} \end{cases}$$

Note that, for a pair of aircraft  $(a, b)$  assigned to a same IAF, when the landing binary variable  $\delta_{ab}$  is equal to 1, then  $a$  should cross the IAF before  $b$ , so that the sequencing variable  $\delta_{ab}$  coherently expresses the relative order between  $a$  and  $b$  on the shared IAF, as required. In the case where  $a$  and  $b$  are not assigned to the same IAF, then  $\delta_{ab}$  is only meaningful for the landing sequence (of interest in the second-stage problem). In comparison with the models proposed in Khassiba et al. (2019, 2020), where the sequencing binary variables mean *direct precedence* between a pair of aircraft like in the classical model for the Traveling Salesman Problem (TSP), here we define the sequencing variables as in scheduling theory, where direct precedence is *not* required. For instance, if  $\delta_{ab} = 1$ , then aircraft  $b$  must land *after*  $a$ , but *not necessarily directly* after  $a$ , i.e., there might be a certain number of aircraft landing after  $a$  and before  $b$ . This holds true, regardless of whether the aircraft are assigned to the same IAF or not. This definition of the sequencing variables  $\delta_{ab}$  allows us to guarantee that the target landing sequence is a coherent merging of the target sequences from all IAFs.

For the sake of simplification, let us assume a fixed rerouting delay from any IAF  $i \in \mathcal{I}$  to any IAF  $j \in \mathcal{I}$ , with the following general notation:

$$r^{ij} = \begin{cases} r > 0 & \text{if } i \neq j \\ 0 & \text{otherwise.} \end{cases} \quad (8)$$

From an operational perspective, a fixed rerouting delay may be justified for example in the case of two IAFs, where the delay can be assumed proportional to the distance between the two IAFs.

Let  $t_a$  and  $x_a$  be two continuous decision variables denoting respectively the *target take-off time* for on-ground aircraft  $a \in \mathcal{A}^G$ , and the *target IAF time* for aircraft  $a \in \mathcal{A}$  (on-ground or airborne). In the following, we detail these target time decision variables according to the flight status: on-ground or airborne.

*On-ground aircraft.* Let  $a \in \mathcal{A}^G$  be an on-ground aircraft. The target take-off time,  $t_a$ , of aircraft  $a$  must lie within an appropriate time window:

$$t_a \in \left[ P_a^{\text{TOT}}, P_a^{\text{TOT}} + \bar{d}^G \right] \quad (9)$$

Given the target take-off time,  $t_a$ , and an unimpeded flight time,  $\hat{V}_a^O$ , from the origin airport of aircraft  $a$  to its initial IAF  $i^*$ , we define the unconstrained IAF time, denoted  $U_a^{O \rightarrow i}$ , for on-ground aircraft  $a$  to reach an assigned IAF  $i \in \mathcal{I}$  (possibly the same as the initial IAF  $i^*$ ) as follows:

$$U_a^{O \rightarrow i} = t_a + r^{i^*i} + \hat{V}_a^O \quad (10)$$

The unconstrained IAF time for an on-ground aircraft  $a$  represents the time at which  $a$  will reach the assigned IAF given that it took off at its target time, and assuming that no disturbances occur in the airspace during the flight. It can also be seen as an update of the predicted time to start the approach phase knowing the take-off time.

Finally, if the on-ground aircraft  $a$  is assigned to IAF  $i \in \mathcal{I}$ , then its target IAF time,  $x_a$ , must lie within an appropriate time window:

$$x_a \in \left[ U_a^{O \rightarrow i} - \underline{d}_a^R, U_a^{O \rightarrow i} + \bar{d}_a^R \right] \quad (11)$$

*Airborne aircraft.* Let  $a \in \mathcal{A}^A$  be an airborne aircraft. The planned IAF time of aircraft  $a$  to reach IAF  $i \in \mathcal{I}$  (possibly the same as its initial IAF  $i^*$ ),  $P_a^i$ , is given by Eq. (3), where  $P_a^{i^*}$  is an input data.

If the airborne aircraft  $a$  is assigned to IAF  $i \in \mathcal{I}$ , then its target IAF time,  $x_a$ , must lie within an appropriate time window:

$$x_a \in \left[ P_a^i - \underline{d}_a^R, P_a^i + \bar{d}_a^R \right] \quad (12)$$

For safety reasons, target IAF times of a pair of successive aircraft crossing the same IAF must be separated by the minimal IAF time separation,  $\underline{S}$ . More precisely, for all pairs of aircraft  $(a, b) \in \mathcal{A} \times \mathcal{A}$ ,  $a \neq b$ , we require that:

$$x_b \geq x_a + \underline{S} \quad \text{if aircraft } a \text{ and } b \text{ are assigned to the same IAF, and } a \text{ is followed by } b. \quad (13)$$

In order to capture the fact that two aircraft are assigned to the same IAF, we introduce an auxiliary binary decision variables  $\phi_{ab}$ , for each pair of aircraft  $(a, b) \in \mathcal{A} \times \mathcal{A}$ ,  $a \neq b$ :

$$\phi_{ab} = \begin{cases} 1 & \text{if aircraft } a \text{ and } b \text{ are both assigned to the same IAF} \\ 0 & \text{otherwise} \end{cases}$$

Note that these binary variables are inspired by the multiple-runway formulation of the aircraft landing problem proposed in Beasley et al. (2000, Section 4).

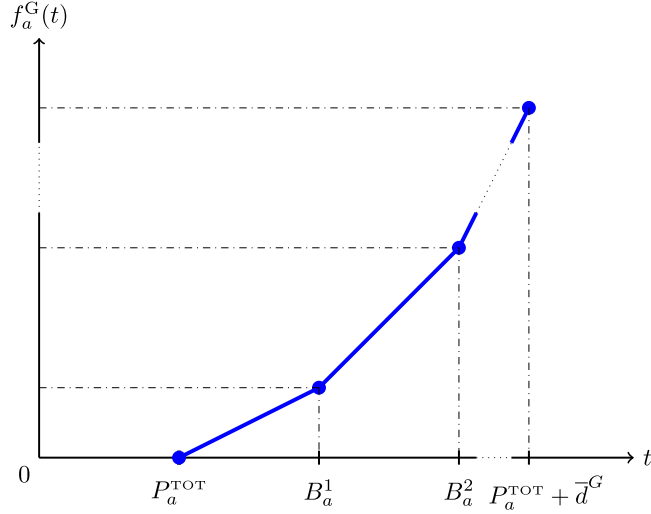


Fig. 3. Convex piecewise linear (at-gate) delay cost function with 2 breakpoints  $B_a^1$ , and  $B_a^2$ .

*First-stage objective function.* In the first stage, we minimize the cost of delay incurred by on-ground aircraft at departure gate. For an on-ground aircraft  $a \in \mathcal{A}^G$ , the at-gate delay can be expressed as  $(t_a - P_a^{\text{TOT}})$ , and according to (9), it is bounded as follows:

$$(t_a - P_a^{\text{TOT}}) \in [0, \bar{d}^G] \quad (14)$$

The cost of the delay at gate of an on-ground aircraft  $a$  can be computed through a delay-cost function, denoted  $f_a^G$ . We assume this delay cost function to be convex and piecewise linear, as sketched in Fig. 3, where the coordinates of the different breakpoints can be based, for instance, on reference delay-cost values reported in Cook and Tanner (2015). Hence, the total delay cost at gate for all on-ground aircraft can be expressed as follows:

$$\sum_{a \in \mathcal{A}^G} f_a^G(t_a - P_a^{\text{TOT}}) \quad (15)$$

We assume that the *actual IAF time* of a given aircraft  $a \in \mathcal{A}$  will deviate, with respect to its target IAF time,  $x_a$ , by a random amount of time, denoted  $\omega_a$ , according to a known probability distribution. Hence, the actual IAF time of an aircraft  $a \in \mathcal{A}$  is  $(x_a + \omega_a)$ , where  $\omega_a$  is a possible realization of the random variable  $\omega_a$ . In the second stage, all random variables are assumed to be revealed, giving rise to a second-stage optimization problem, that we formulate in the next subsection.

### 3.2. Second-stage problem

In the second stage, we seek to determine a *target landing time* for each aircraft, given that the target landing sequence is already found in the first stage. Consider an aircraft  $a \in \mathcal{A}$ . Let  $y_a$  denote the *target landing time* for aircraft  $a$ , which plays the role of the second-stage decision variable for aircraft  $a$ . Given that the actual time of aircraft  $a$  to cross its assigned IAF  $i \in \mathcal{I}$  is  $(x_a + \omega_a)$ , and that minimal and maximal flight times from IAF  $i$  to touch down are  $\underline{V}_a^i$  and  $\bar{V}_a^i$  respectively, then we can compute the landing time window that the target landing time  $y_a$  must satisfy:

$$y_a \in [E_a^L(\omega_a, i), L_a^L(\omega_a, i)] \quad (16)$$

where:

$$E_a^L(\omega_a, i) = (x_a + \omega_a) + \underline{V}_a^i \quad (17)$$

$$L_a^L(\omega_a, i) = (x_a + \omega_a) + \bar{V}_a^i \quad (18)$$

Note that  $E_a^L(\omega_a, i)$  and  $L_a^L(\omega_a, i)$  are realizations of the random variables  $E_a^L(\omega_a, i)$  and  $L_a^L(\omega_a, i)$  that depend on the random time deviation,  $\omega_a$ . Hence, landing time windows are only known with certainty at the second stage. Also, according to the value of the decision variable  $x_a$  and the realization  $\omega_a$ , one expects that  $P_a^L \in [E_a^L(\omega_a, i), L_a^L(\omega_a, i)]$ , may or may not hold. Typically, in case of a long delay in the en-route phase, the planned landing time  $P_a^L$  may become infeasible for some realizations of  $\omega_a$ , i.e.,  $P_a^L < E_a^L(\omega_a, i) < L_a^L(\omega_a, i)$ .

Operational constraints related to final-approach separations that must be satisfied between any pair of successively landing aircraft  $(a, b) \in \mathcal{A} \times \mathcal{A}$ ,  $a \neq b$ , can be expressed as follows:

$$y_b \geq y_a + S_{ab} \quad \text{if aircraft } a \text{ lands before } b, \quad (19)$$



where  $S_{ab}$  is the minimum final-approach separation between the leading aircraft  $a \in \mathcal{A}$  and the following aircraft  $b \in \mathcal{A}$ . Values of  $S_{ab}$  are given in Table 1, according to each aircraft's wake-turbulence category.

*Second-stage objective function.* In the second stage, we minimize the cost of time deviation (delay and advance) incurred during the en-route and approach phases for all aircraft. The actual IAF time of an airborne aircraft  $a \in \mathcal{A}^A$  assigned to an IAF  $i \in \mathcal{I}$  may deviate from the planned IAF time of  $a$  at its initial IAF  $i^*$ ,  $P_a^{i^*}$ , within the following interval:

$$x_a + \omega_a - P_a^{i^*} \in \left[ \omega_a + r^{i^*i} - \underline{d}_a^R, \omega_a + r^{i^*i} + \overline{d}_a^R \right] \quad (20)$$

Remark that the lower bound  $(\omega_a + r^{i^*i} - \underline{d}_a^R)$  may be non-positive even if  $\underline{d}_a^R = 0$ , due to a large negative  $\omega_a < 0$ . That is to say that, because of uncertainty, an aircraft can be in advance compared with its initial IAF planned time ( $x_a + \omega_a < P_a^{i^*}$ ), even if we do not allow expediting aircraft in the en-route phase.

The expressions of delay and of time advance during the en-route phase for an airborne aircraft  $a \in \mathcal{A}^A$  read respectively:

$$\max \left( 0, x_a + \omega_a - P_a^{i^*} \right) \quad \text{and} \quad - \min \left( 0, x_a + \omega_a - P_a^{i^*} \right) \quad (21)$$

The actual IAF time of an on-ground aircraft  $a \in \mathcal{A}^G$  assigned to an IAF  $i \in \mathcal{I}$  may deviate from its unconstrained IAF time at its initial IAF  $i^*$ ,  $U_a^{O \rightarrow i^*}$ , within the following interval:

$$x_a + \omega_a - U_a^{O \rightarrow i^*} = x_a + \omega_a - (t_a + \hat{V}_a^O) \in \left[ \omega_a + r^{i^*i} - \underline{d}_a^R, \omega_a + r^{i^*i} + \overline{d}_a^R \right] \quad (22)$$

A remark similar to that on the interval (20) applies for on-ground aircraft. For an on-ground aircraft  $a \in \mathcal{A}^G$ , delay and of time advance during the en-route phase can be expressed similarly to those in (21). Let us define the unconstrained landing time, denoted  $U_a^i$ , of aircraft  $a$  from IAF  $i$  as the landing time of that aircraft assuming it starts its approach phase from IAF  $i$ , and that there is no other aircraft in the terminal area:

$$U_a^i = x_a + \omega_a + \hat{V}_a^i \quad (23)$$

The target landing time  $y_a$  of an aircraft  $a$  assigned to IAF  $i$  may deviate from its unconstrained landing time  $U_a^i$  within the following interval:

$$y_a - U_a^i \in \left[ -\underline{d}_a^T, \overline{d}_a^T \right] \quad (24)$$

Consider an aircraft  $a \in \mathcal{A}$  (either initially on-ground or airborne at the moment when making first-stage decisions) coming from IAF  $i$ . Delay and advance times during the approach phase of aircraft  $a \in \mathcal{A}$  from IAF  $i$  can be expressed similarly to those in (21).

Let  $f_a^R$  and  $f_a^T$  denote the cost functions of time deviation incurred during the en-route and the approach phases for an aircraft  $a$  respectively. These cost functions are assumed to be convex and piecewise linear. Fig. 4 depicts  $f_a^R$  for an airborne aircraft  $a \in \mathcal{A}^A$ . The total cost during the en-route and the approach phases for all aircraft can be expressed as follows:

$$\sum_{a \in \mathcal{A}^G} f_a^R(x_a + \omega_a - (t_a + \hat{V}_a^O)) + \sum_{a \in \mathcal{A}^A} f_a^R(x_a + \omega_a - P_a^{i^*}) + \sum_{a \in \mathcal{A}} f_a^T(y_a - (x_a + \omega_a + \hat{V}_a^i)) \quad (25)$$

In the next subsection, we present the full two-stage stochastic programming model of the first variant.

### 3.3. Full two-stage stochastic model for the first variant

Let us introduce the following additional notations:

- $\mathcal{A}^{i^*}$ : index set of aircraft whose initial IAF is  $i^* \in \mathcal{I}$
- $\mathcal{A}^{i^*,G}$ : index set of on-ground aircraft whose initial IAF is  $i^* \in \mathcal{I}$
- $\mathcal{A}^{i^*,A}$ : index set of airborne aircraft whose initial IAF is  $i^* \in \mathcal{I}$

We have the following relationships:

- For every  $i \in \mathcal{I}$ :  $\mathcal{A}^i = \mathcal{A}^{i,G} \cup \mathcal{A}^{i,A}$ , and  $\mathcal{A}^{i,G} \cap \mathcal{A}^{i,A} = \emptyset$
- For every pair  $(i, j) \in \mathcal{I} \times \mathcal{I}$ , such that  $i \neq j$ :

- $\mathcal{A}^G = \bigcup_{i \in \mathcal{I}} \mathcal{A}^{i,G}$ , and  $\mathcal{A}^{i,G} \cap \mathcal{A}^{j,G} = \emptyset$
- $\mathcal{A}^A = \bigcup_{i \in \mathcal{I}} \mathcal{A}^{i,A}$ , and  $\mathcal{A}^{i,A} \cap \mathcal{A}^{j,A} = \emptyset$

The two-stage stochastic programming model of the extended aircraft arrival management problem under uncertainty with multiple IAFs, and where IAF assignment is considered as a first-stage decision, reads:

$$\min_{\zeta, \phi} \sum_{a \in \mathcal{A}^G} f_a^G(t_a - P_a^{\text{TOT}}) + \mathbb{E}_\omega[Q(\zeta, \delta, t, x, \omega)] \quad (26)$$

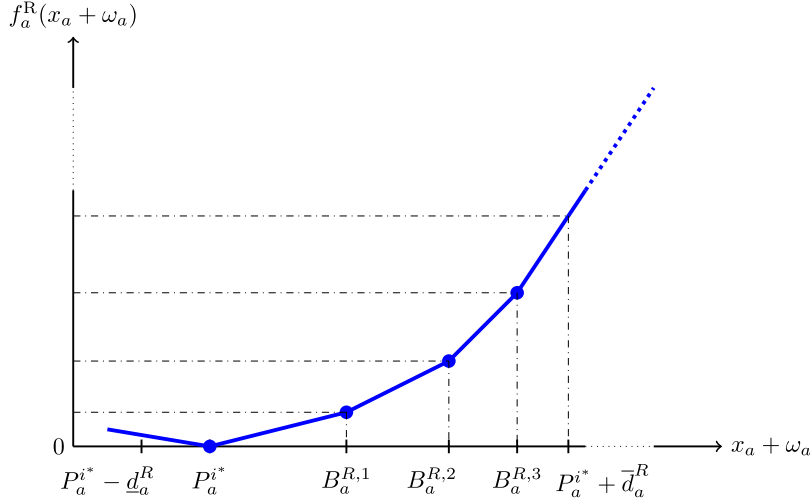


Fig. 4. Convex piecewise-linear (en-route) cost function with 4 breakpoints  $P_a^{i^*}$ ,  $B_a^{R,1}$ ,  $B_a^{R,2}$ , and  $B_a^{R,3}$ .

$$\text{s.t. } \sum_{i \in I} \zeta_{ai} = 1 \quad a \in \mathcal{A} \quad (27)$$

$$\phi_{ab} = \phi_{ba} \quad (a, b) \in \mathcal{A} \times \mathcal{A}, \quad a < b \quad (28)$$

$$\phi_{ab} \geq \zeta_{ai} + \zeta_{bi} - 1 \quad i \in I, \quad (a, b) \in \mathcal{A} \times \mathcal{A}, \quad a < b \quad (29)$$

$$\delta_{ab} + \delta_{ba} = 1 \quad (a, b) \in \mathcal{A} \times \mathcal{A}, \quad a < b \quad (30)$$

$$x_b \geq x_a + \underline{S} - M_{ab}(2 - \phi_{ab} - \delta_{ab}) \quad (a, b) \in \mathcal{A} \times \mathcal{A}, \quad a \neq b \quad (31)$$

$$-\bar{d}_a^R \leq x_a - t_a - \hat{V}_a^O - \sum_{j \in I} r^{i^*j} \zeta_{aj} \leq \bar{d}_a^R \quad i^* \in I, \quad a \in \mathcal{A}^{i^*G} \quad (32)$$

$$-\bar{d}_a^R \leq x_a - P_a^{i^*} - \sum_{j \in I} r^{i^*j} \zeta_{aj} \leq \bar{d}_a^R \quad i^* \in I, \quad a \in \mathcal{A}^{i^*A} \quad (33)$$

$$0 \leq t_a - P_a^{\text{TOT}} \leq \bar{d}_a^G \quad a \in \mathcal{A}^G \quad (34)$$

$$\zeta_{ai} \in \{0, 1\} \quad i \in I, \quad a \in \mathcal{A} \quad (35)$$

$$\phi_{ab} \in \{0, 1\} \quad (a, b) \in \mathcal{A} \times \mathcal{A}, \quad a \neq b \quad (36)$$

$$\delta_{ab} \in \{0, 1\} \quad (a, b) \in \mathcal{A} \times \mathcal{A}, \quad a \neq b \quad (37)$$

where:

$$Q(\zeta, \delta, t, x, \omega) = \min_y \sum_{a \in \mathcal{A}^G} f_a^R(x_a + \omega_a - (t_a + \hat{V}_a^O)) + \sum_{a \in \mathcal{A}^A} f_a^R(x_a + \omega_a - P_a^{i^*}) + \sum_{a \in \mathcal{A}} f_a^T\left(y_a - \left(x_a + \omega_a + \sum_{i \in I} \hat{V}_a^i \zeta_{ai}\right)\right) \quad (38)$$

$$\text{s.t. } y_b \geq y_a + S_{ab} - M_{ab}^L(1 - \delta_{ab}) \quad (a, b) \in \mathcal{A} \times \mathcal{A}, \quad a \neq b \quad (39)$$

$$\sum_{i \in I} \bar{V}_a^i \zeta_{ai} \leq y_a - (x_a + \omega_a) \leq \sum_{i \in I} \bar{V}_a^i \zeta_{ai} \quad a \in \mathcal{A} \quad (40)$$

where  $M_{ab}$  and  $M_{ab}^L$  are sufficiently large (so-called big-M) constants defined for all  $(a, b) \in \mathcal{A} \times \mathcal{A}$ ,  $a \neq b$ , helping to enable/disable separation constraints at IAFs and at the runway, respectively. The objective function (26) involves minimizing the sum of the total at-gate delay cost and the expectation of the second-stage objective function. Constraints (27) ensure that each aircraft is assigned to exactly one IAF. Constraints (28) express the symmetry of the auxiliary variables  $\phi_{ab}$ 's. Constraints (29) ensure the logical coherence of the decision variables  $\phi_{ab}$ 's and the IAF assignment variables  $\zeta_{ai}$ 's. Constraints (30) express the logical order between any pair of aircraft. Constraints (31) ensure separation between target IAF times of any pair of successive aircraft assigned to the same IAF. The big-M constant  $M_{ab}$  can be set to:

$$M_{ab} = L_a^{\text{best}} - E_b^{\text{best}} + \underline{S} \quad (41)$$

**Table 3**

Expressions of the constants  $E_b^{\text{best}}$  and  $L_a^{\text{best}}$  that occur in the definition of the big-M constant  $M_{ab}$  according to flight status (case where IAF assignment is a first-stage decision).

Flight status	On-ground (in $\mathcal{A}^G$ )	Airborne (in $\mathcal{A}^A$ )
$E_b^{\text{best}}$	$P_b^{\text{TOT}} + \hat{V}_b^O - \underline{d}_b^R$	$E_b^{j^*}$ , where $j^*$ is the initial IAF of $b$
$L_a^{\text{best}}$	$P_a^{\text{TOT}} + \overline{d}_a^G + \hat{V}_a^O + r + \overline{d}_a^R$	$L_a^k$ , where $k \in I \setminus \{i^*\}$ is an IAF <i>different</i> from the initial IAF $i^*$ of $a$

**Table 4**

Expressions of the constants  $E_b^{L,\text{best}}$  and  $L_a^{L,\text{best}}$  that occur in the definition of the big-M constant  $M_{ab}^L$  according to flight status (case where IAF assignment is a first-stage decision).

Flight status	On-ground (in $\mathcal{A}^G$ )	Airborne (in $\mathcal{A}^A$ )
$E_b^{L,\text{best}}$	$P_b^{\text{TOT}} + \hat{V}_b^O - \underline{d}_b^R + \omega_b + \min_{k \in I} \{ \underline{V}_b^k + r^{i^*k} \}$ where $j^* \in I$ is the initial IAF of aircraft $b$	$P_b^{j^*} - \underline{d}_b^R + \omega_b + \min_{k \in I} \{ \underline{V}_b^k + r^{i^*k} \}$
$L_a^{L,\text{best}}$	$P_a^{\text{TOT}} + \overline{d}_a^G + \hat{V}_a^O + \overline{d}_a^R + \omega_a + \max_{k \in I} \{ \overline{V}_a^k + r^{i^*k} \}$ where $i^* \in I$ is the initial IAF of aircraft $a$	$P_a^{i^*} + \overline{d}_a^R + \omega_a + \max_{k \in I} \{ \overline{V}_a^k + r^{i^*k} \}$

where:

- $L_a^{\text{best}}$  is the “best” possible upper bound for  $x_a$ , *i.e.*, the smallest upper bound for  $x_a$ , and
- $E_b^{\text{best}}$  is the “best” possible lower bound to  $x_b$ , *i.e.*, the largest lower bound for  $x_b$ ,

while the IAFs assigned to aircraft  $a$  and  $b$  are still unknown. Expression (41) is based on the fact that  $M_{ab}$  should be an upper bound for  $(x_a - x_b + \underline{S})$ . Explicit expressions of  $L_a^{\text{best}}$  and  $E_b^{\text{best}}$  are given in Table 3 according to the flight status (proofs are given in Appendix A).

Note that for a given aircraft  $a \in \mathcal{A}$  (on-ground or airborne),  $E_a^{\text{best}}$  and  $L_a^{\text{best}}$  can also be used to bound the target IAF time  $x_a$ .

Constraints (32) enforce the target IAF time of an on-ground aircraft, with an initial IAF  $i^* \in I$ , to lie within an appropriate time window that depends on the target take-off time and the assigned IAF. Constraints (33) enforce the target IAF time of an airborne aircraft, with an initial IAF  $i^* \in I$ , to lie within an appropriate time window that depends on the planned IAF time and the assigned IAF. Constraints (34) ensure that the target take-off time of an on-ground aircraft is chosen in the appropriate time window. Constraints (35), (36), and (37) stipulate the binary nature of decision variables  $\zeta_{ai}$ 's,  $\phi_{ab}$ 's and  $\delta_{ab}$ 's.

The optimal value of the second-stage problem is noted  $Q(\zeta, \delta, t, x, \omega)$ . The objective function in (38) is the total time-deviation (delay and advance) cost (to be minimized) during the en-route and the approach phases. Constraints (39) ensure final-approach separation between any pair of landing aircraft, where the big-M constant  $M_{ab}^L$  can be set to:

$$M_{ab}^L = L_a^{L,\text{best}} - E_b^{L,\text{best}} + S_{ab} \quad (42)$$

where:

- $L_a^{L,\text{best}}$  is the “best” possible upper bound for  $y_a$ , *i.e.*, the smallest upper bound to  $y_a$ , and
- $E_b^{L,\text{best}}$  is the “best” possible lower bound for  $y_b$ , *i.e.*, the largest lower bound to  $y_b$ ,

while the IAFs assigned to aircraft  $a$  and  $b$  are still unknown. Expression (42) is based on the fact that  $M_{ab}^L$  should be an upper bound for  $(y_a - y_b + S_{ab})$ . Explicit expressions of  $L_a^{L,\text{best}}$  and  $E_b^{L,\text{best}}$  are given in Table 4 according to the flight status (proofs are given in Appendix A).

Note that for a given aircraft  $a \in \mathcal{A}$  (on-ground or airborne),  $E_a^{L,\text{best}}$  and  $L_a^{L,\text{best}}$  can also be used to bound the target landing time  $y_a$ .

Constraints (40) enforce the flight time, for a given aircraft, between its assigned IAF and the runway, to lie within an appropriate flight time window.

#### 4. Second-variant model: IAF assignment as a problem input

In the previous section, we presented a two-stage stochastic programming model for the general case of the extended aircraft arrival management problem, where IAF assignment is considered as a first-stage decision. From an operational viewpoint, as presented in the problem statement (Section 2), IAF changes are usually issued after a modification of the landing runway, or due to unexpected adverse weather in the neighborhood of some IAFs. Also, IAF assignment may be updated to balance aircraft flows among

**Table 5**

Expressions of the constants  $E_b^{\text{best}}$  and  $L_a^{\text{best}}$  that occur in the expression of the big-M constant  $M_{ab}^L$  according to flight status (case where IAF assignment is fixed).

Flight status	On-ground (in $\mathcal{A}^G$ )	Airborne (in $\mathcal{A}^A$ )
$E_b^{\text{best}}$	$P_b^{\text{TOT}} + \hat{V}_b^O - \underline{d}_b^R$	$E_b^*$ (input data)
$L_a^{\text{best}}$	$P_a^{\text{TOT}} + \overline{d}_a^G + \hat{V}_a^O + \overline{d}_a^R$	$L_a^*$ (input data)

IAFs, thereby avoiding long delays at approach. Given that we consider a single runway, and assuming normal weather conditions and relatively-balanced aircraft flows on the IAFs, it is, then, interesting to consider also the realistic case where IAF assignment is given and fixed. Consequently, in this section, we consider the problem variant where initial IAFs pre-assigned to aircraft, 2–3 h before landing, cannot be changed. In this variant, the two-stage stochastic programming model, presented in Section 3, simplifies as follows:

$$\min_{\delta, t, x} \sum_{a \in \mathcal{A}^G} f_a^G(t_a - P_a^{\text{TOT}}) + \mathbb{E}_\omega[Q(\delta, t, x, \omega)] \quad (43)$$

$$\text{s.t. } \delta_{ab} + \delta_{ba} = 1 \quad (a, b) \in \mathcal{A} \times \mathcal{A}, \quad a < b \quad (44)$$

$$x_b \geq x_a + \underline{S} - M_{ab}(1 - \delta_{ab}) \quad i^* \in \mathcal{I}, (a, b) \in \mathcal{A}^{i^*} \times \mathcal{A}^{i^*}, \quad a \neq b \quad (45)$$

$$-\underline{d}_a^R \leq x_a - (t_a + \hat{V}_a^O) \leq \overline{d}_a^R \quad i^* \in \mathcal{I}, a \in \mathcal{A}^{i^*, G} \quad (46)$$

$$-\underline{d}_a^R \leq x_a - P_a^{i^*} \leq \overline{d}_a^R \quad i^* \in \mathcal{I}, a \in \mathcal{A}^{i^*, A} \quad (47)$$

$$0 \leq t_a - P_a^{\text{TOT}} \leq \overline{d}_a^G \quad a \in \mathcal{A}^G \quad (48)$$

$$\delta_{ab} \in \{0, 1\} \quad (a, b) \in \mathcal{A} \times \mathcal{A}, \quad a \neq b \quad (49)$$

where:

$$Q(\delta, t, x, \omega) = \min_y \sum_{a \in \mathcal{A}^G} f_a^R(x_a + \omega_a - (t_a + \hat{V}_a^O)) + \sum_{a \in \mathcal{A}^A} f_a^R(x_a + \omega_a - P_a^{i^*}) + \sum_{a \in \mathcal{A}} f_a^T(y_a - (x_a + \omega_a + \hat{V}_a^{i^*})) \quad (50)$$

$$\text{s.t. } y_b \geq y_a + S_{ab} - M_{ab}^L(1 - \delta_{ab}) \quad (a, b) \in \mathcal{A} \times \mathcal{A}, \quad a \neq b \quad (51)$$

$$\underline{V}_a^{i^*} \leq y_a - (x_a + \omega_a) \leq \overline{V}_a^{-i^*} \quad i^* \in \mathcal{I}, a \in \mathcal{A}^{i^*} \quad (52)$$

The main simplifications are as follows. When IAF assignment is fixed, there is no more need for the IAF assignment decision variables  $\zeta_{ai}$ 's, nor for the decision variables  $\phi_{ab}$ 's, identifying whether two aircraft are assigned to the same IAF or not. Also, with respect to the first-variant model, IAF separation constraints (31), IAF time-window constraints (32) and (33), and runway time-window constraints (40) are updated into constraints (45), (46), (47), and (52) respectively. In the following, we comment in detail the model of this second variant.

Note that first-stage decision variables are now limited to  $\delta_{ab}$ 's,  $t_a$ 's, and  $x_a$ 's. The objective function (43) and constraints (44) are similar to their counterparts of the first variant, (26) and (30) respectively. The IAF separation constraints (45) are expressed only for pairs of aircraft crossing the same IAF, *i.e.*, pairs of aircraft from the same subset  $\mathcal{A}^{i^*}$ , for  $i^* \in \mathcal{I}$ . For a pair  $(a, b) \in \mathcal{A} \times \mathcal{A}$ ,  $a \neq b$ , the big-M constants  $M_{ab}$ 's in constraints (45) can be set as in Eq. (41), while  $E_b^{\text{best}}$  and  $L_a^{\text{best}}$  are defined as follows:

- $L_a^{\text{best}}$  is the “best”, *i.e.*, the smallest, upper bound for  $x_a$ .
- $E_b^{\text{best}}$  is the “best”, *i.e.*, the largest, lower bound for  $x_b$ .

Explicit expressions of  $L_a^{\text{best}}$  and  $E_b^{\text{best}}$  are given in Table 5 according to the flight status (proofs are given in Appendix A).

For each aircraft, the IAF is known in advance, hence the IAF time window is known without ambiguity. Then, IAF time-window constraints (46) and (47) are formulated straightforwardly. Time-window constraints on target take-off times (48) are identical to their counterparts (34) in the first-variant model. Constraints (49), similarly to (37) in the first-variant model, stipulate the binary nature of the sequencing variables  $\delta_{ab}$ 's.

For the second-stage problem,  $Q(\delta, t, x, \omega)$  stands for its optimal value. In the objective function (50), the expression of the unconstrained flight time from the IAF to the runway involved in the approach delay cost function simplifies, compared to (38), since IAFs are known in advance. Runway-separation constraints (51) are similar to their counterparts (39) of the first-variant model, while the big-M constant  $M_{ab}^L$  can be set to:

$$M_{ab}^L = \left( L_a^{\text{best}} + \omega_a + \overline{V}_a^{i^*} \right) - \left( E_b^{\text{best}} + \omega_b + \underline{V}_b^{j^*} \right) + S_{ab}, \quad (53)$$

where explicit expressions for  $E_b^{\text{best}}$  and  $L_a^{\text{best}}$  are given in Table 5, and  $i^*$  and  $j^*$  are the initial IAFs of aircraft  $a$  and  $b$  respectively. The expression (53) can be obtained as follows. The big-M constant  $M_{ab}^L$  is required to be an upper bound for  $(y_a - y_b + S_{ab})$ . We have:  $y_a \leq x_a + \omega_a + \bar{V}_a^{i^*} \leq L_a^{\text{best}} + \omega_a + \bar{V}_a^{i^*}$ . A similar reasoning can be made to upper bound  $(-y_b)$ .

Finally, landing time-window constraints (52) simplify (compared to their counterparts (40), of the first-variant model) using the fact that the minimal and the maximal flight times for each aircraft, from the pre-assigned IAF to the runway, are known in advance.

## 5. Notes on the proposed models and on the solution method

In two-stage stochastic programming, the first-stage solution directly impacts the definition of the second-stage problem, and thus its feasibility region. When for each feasible first-stage solution, there is, at least, one feasible second-stage solution, for almost any realization of the uncertainty; the two-stage stochastic programming model is said to have a *relatively complete recourse*. Formal definitions of different recourse types can be found, for example, in Birge and Louveaux (2011, Chapter 3). This property is convenient because it guarantees that the first-stage solution can be safely implemented, for almost any realization of the uncertainty.

In this section, we show that the recourse in our problem is *not* relatively complete. Despite the loss of this property in theory, realistic problem parameters, as those used in our numerical study, guarantee the feasibility of the second-stage problem, as shown in Section 5.1. The two-stage stochastic programming models presented in Sections 3 and 4 involve convex piecewise-linear functions, that we linearize by introducing extra continuous variables using the standard *incremental cost* technique (Keha et al., 2004). The expectancy operator, appearing in the objective functions, can be handled through *Sample Average Approximation* (SAA) as presented in Section 5.2.

### 5.1. Recourse type

In our context, the relatively-complete recourse property can be interpreted as follows: for any schedule at the IAFs and any landing sequence, feasible for the first-stage problem, we are able to find feasible landing times, for (almost) any IAF time deviations (i.e., for almost any realization of the random variables) by solving the corresponding second-stage problem. The presence of time-window constraints for landing (in the second-stage problem) may prevent satisfying the landing sequence (determined in the first stage) once uncertainty is revealed. For instance, consider aircraft  $a$  and  $b$  assigned to the same IAF, such that aircraft  $a$  is scheduled to reach the IAF before aircraft  $b$ , i.e.,  $x_b \geq x_a + \underline{S}$ . According to the definition of the sequencing variables, aircraft  $a$  should also land before aircraft  $b$ . Consider the IAF time deviations  $\omega_a$  and  $\omega_b$ , such that:  $x_b + \omega_b < x_a + \omega_a$ . In this uncertainty scenario, the relative order of aircraft  $a$  and  $b$  is inverted when reaching their IAF. If the landing time windows are very tight, it will not be possible to recover the target relative order of aircraft  $a$  and  $b$  for landing. Hence, the second-stage problem becomes infeasible, for the target landing sequencing computed beforehand in the first stage. Consequently, the two-stage stochastic programming models, proposed in this paper, do *not* have a *relatively complete recourse*. A similar example is given in Khassiba et al. (2020), where the proposed model has the same type of recourse. However, in practice, when landing time windows are large “enough”, one can find target landing times that satisfy any landing sequence determined in the first stage, for (almost) any IAF time deviations. In our numerical experiments, presented in Section 6, infeasible second-stage problems, for fixed first-stage solutions, were not observed.

### 5.2. Sample average approximation

We assume that deviations of IAF times,  $\omega_a$ ,  $a \in \mathcal{A}$ , are independent and identically distributed, each according to a normal distribution with mean zero, and standard deviation  $\sigma$ . Due to this continuous distribution, and to the fact that  $Q(\delta, t, x, \omega)$  is the optimal value of a linear program, a closed-form expression for  $\mathbb{E}_\omega [Q(\delta, t, x, \omega)]$  is often difficult, and even impossible, to find in the general case (Shapiro et al., 2021, Chapter 5). The expectancy operator in the objective function can be handled by the method of Sample Average Approximation (SAA) (Fu et al., 2015), that constructs an *approximate problem* using a finite set of  $n_S$  second-stage scenarios. One scenario corresponds to one possible realization of the random vector  $\omega$ , i.e., one possible time deviation in the en-route phase for each aircraft. To construct an approximate problem, we start by generating (sampling)  $n_S$  independent scenarios using Monte-Carlo method. Then, we formulate  $n_S$  second-stage problems, each corresponding to one scenario. We approximate the expectation of the second-stage optimal value,  $\mathbb{E}_\omega [Q(\delta, t, x, \omega)]$ , by a *sample average* over the  $n_S$  sampled scenarios:  $\frac{1}{n_S} \sum_{s=1}^{n_S} Q(\delta, t, x, \omega^s)$ , where  $\omega^s = (\omega_1^s, \omega_2^s, \dots, \omega_n^s)$  corresponds to the realization of the random vector  $\omega$  in scenario  $s$ . The first-stage problem, together with the  $n_S$  copies of the second-stage problem, unified under one linear objective function give rise to a (possibly large) single-stage mixed-integer linear program, that can be solved by a commercial MILP solver. We call the solution of the approximate problem, noted  $(\delta_{SP}, t_{SP}, x_{SP})$ , the *stochastic solution*.

On the other hand, we formulate the so-called *expected value problem*, that corresponds to a specific approximate deterministic problem which has only one scenario in the second stage: the *mean scenario*. The mean scenario corresponds to no deviations in IAF time for all aircraft, i.e., every aircraft arrives at its assigned IAF, exactly on its target time. We call the solution of the expected value problem, noted  $(\delta_{EV}, t_{EV}, x_{EV})$ , the *deterministic solution*.

In order to compare the quality of both solutions (the stochastic and the deterministic solutions), we sample  $n_{S_v}$  ( $\gg n_S$ ) additional and independent scenarios that we use as a *reference scenario tree*, as named in Kaut and Wallace (2007). We then formulate the *validation problem*: an approximate problem whose scenario set corresponds to the sampled reference scenario tree. We evaluate both solutions on this reference tree, and we call the obtained objective-function values, the *validation scores*. Let  $v_{SP}$  denote the

**Table 6**  
Instance statistics.

Instance Id	10_559_618	10_607_623	10_619_634	10_624_640	10_634_659
# Aircraft ( $n$ )	10	10	10	10	10
First Planned Landing	6:10:46	6:14:46	6:20:30	6:23:18	6:28:06
Last Planned Landing	6:21:16	6:23:28	6:29:00	6:31:22	6:40:35
Time span	10 min 30 s	8 min 42 s	8 min 30 s	8 min 4 s	12 min 29 s
# Airborne ( $n_A$ )	6	4	3	5	7
# On-ground ( $n_G$ )	4	6	7	5	3
# Medium (M)	4	6	7	7	7
# Heavy (H)	6	4	3	3	3
# assigned to IAF 1	6	5	5	4	3
# assigned to IAF 2	4	5	5	6	7

validation score of the stochastic solution, and  $v_{EV}$  the validation score of the deterministic solution. Note that  $v_{SP}$  expresses the expected cost of time deviation (delay and advance), if the stochastic solution is implemented, while  $v_{EV}$  expresses the expected cost, if the deterministic solution is implemented.

The difference between the two validation scores,  $v_{SP}$  and  $v_{EV}$ , is called the *value of the stochastic solution*, denoted VSS and expressed as follows:

$$VSS = v_{SP} - v_{EV} \quad (54)$$

The *relative VSS* is computed as the ratio:

$$relative\ VSS\ (\%) = \frac{v_{SP} - v_{EV}}{v_{EV}} \quad (55)$$

The value of the stochastic solution quantifies the benefit from taking into account the probability distribution of IAF deviation times, through two-stage stochastic programming. More specifically, VSS measures, hopefully, the expected cost saving, when the solution applied to the extended aircraft arrival problem is the one provided by our two-stage stochastic models, and not by its uncertainty-unaware counterpart.

## 6. Computational study

Sections 3 and 4 presented two-stage stochastic programming models for two variants of the extended aircraft arrival management problem with multiple IAFs. The first variant, presented in Section 3, corresponds to the general case where IAF assignment is a first-stage decision, while the second variant, formulated in Section 4, deals with a realistic special case where IAF assignment is fixed in advance.

In this section, we report a computational study conducted on five instances, each of which involves 10 aircraft and two IAFs. Four levels of uncertainty are tested. Instances and test data are described in Section 6.1. The two problem variants, referred to as “IAF (assignment) as a decision”, and “IAF as an input” are studied. In this computational study, we consider that no time advance is possible when aircraft are still at gate and when they are in the approach phase. Preliminary experiments, reported in Section 6.2, show that time advance in the en-route phase can significantly decrease the delay cost compared to the case where no advance is possible. As a consequence, this computational study focuses solely on the case where time advance is allowed in the en-route phase. Summary results are reported in Section 6.3. The value of the stochastic solution is studied in Section 6.4. The effect of flexible IAF assignment is analyzed in Section 6.5. Finally, a more detailed analysis on the instance featuring the highest VSS is given in Section 6.6.

All results are obtained with a Python 2.7 code and IBM ILOG CPLEX 12.7.1 run on a Linux platform with eight 2.66 GHz Xeon processors and 32 GB of RAM.

### 6.1. Instances and test data

We use realistic data from Paris CDG airport consisting of 30 aircraft planning to land on the northern runway 27R, and to cross the IAFs, between 5:59 AM and 6:59 AM, on May 5th, 2015. In order to experiment on a highly congested situation, this schedule is compressed by a factor of two, so that the time span becomes 30 min. Initially, 14 aircraft were assigned to MOPAR, 14 other aircraft to LORNI, and two aircraft to OKIPA. We updated the IAF of the last two aircraft to IAF LORNI (the closest IAF to OKIPA), in order to build an instance with only  $m = 2$  IAFs, and involving a more balanced number of aircraft on the IAFs.

We divide the 30-aircraft instance into five instances of  $n = 10$  aircraft each. The first instance considers the first 10 aircraft. The second instance moves forward with 5 aircraft, and considers the next 10 aircraft, starting from the 6th aircraft to the 15th aircraft. Likewise, we build three more instances moving forward with 5 aircraft each time. Some statistics about these five instances are given in Table 6, and more details are given in Table B.1 in Appendix B.

**Table 7**  
Maximal possible time advance and delay (in seconds) by flight phase, for any  $a \in \mathcal{A}$ .

At-gate <sup>a</sup>	En-route		Approach	
Max delay	Max advance	Max delay	Max advance	Max delay
$\bar{d}_a^G = 900$	$\bar{d}_a^R = 60$	$\bar{d}_a^R = 300$	$\bar{d}_a^T = 0$	$\bar{d}_a^T = 1200$

<sup>a</sup>At-gate delay can be applied only to aircraft initially on-ground,  $a \in \mathcal{A}^G$ , when making first-stage decisions.

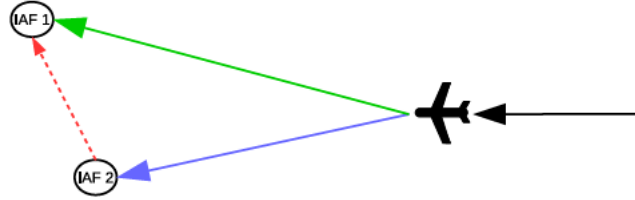


**Fig. 5.** Initial (in blue), new (in green), and inter-IAF distances (in dashed red). By the triangle inequality, the new distance is longer than the initial one by less than the inter-IAF distance. (For interpretation of the references to color in this figure legend, the reader is referred to the web version of this article.)

**Table 8**  
Unconstrained flight times (in seconds) from each IAF to runway 27R for any  $a \in \mathcal{A}$ .

IAF	RWY	Unconst. flight time
1 (MOPAR)	27R	$\hat{V}_a^1 = 780$
2 (LORNI)	27R	$\hat{V}_a^2 = 660$

**Maximal possible time advance and maximal possible delay.** In this computational study, we consider that maximal possible time advance and delay are the same for all aircraft type. They only depend on the flight phase. Advance and delay values (in seconds) are given in Table 7.

**Flight times from each IAF to the runway.** Unconstrained flight time from each IAF to the runway is assumed to be aircraft independent, and are shown in Table 8.

**Rerouting time to change IAF.** We set  $r = 300$  s (5 min). The rationale of this choice is as follows. The distance between MOPAR (IAF 1) and LORNI (IAF 2) is around 66.68 NM. Assuming ground speed in the cruise phase of 450 knots (NM/hour), then the time to fly from one IAF to the other is  $\bar{r} = 8$  min and 53 s. In our problem setup, we assume that the instruction of changing the IAF is issued 2 to 3 h before landing. Hence, the concerned aircraft can change its route early enough so that it is delayed by  $r < \bar{r}$ , as sketched in Fig. 5.

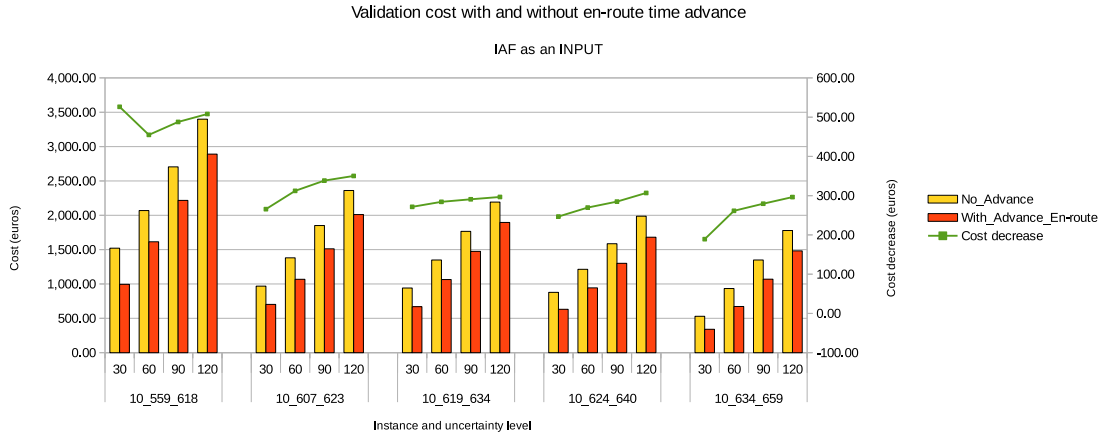
**Minimal time separations.** The minimal time separation on each IAF is  $\underline{S} = 72$  s, like in Khassiba et al. (2019, 2020). Final-approach time separations are specified in Table 1.

**Random IAF time deviations.** In our context, we assume that uncertainty corresponds to the accuracy of meeting an IAF target time, e.g., required time of arrival to IAF. Such a setting was considered in Lee (2008), where accuracy is related to the quality of on-board equipments. The author used a symmetric triangular distribution with a range  $\pm 150$  s, for aircraft equipped with an accurate Flight Management System (FMS), and with a range  $\pm 300$  s for less appropriately equipped aircraft. By choosing a normal distribution with a standard deviation ranging from 30 to 120 s, IAF time deviations fall more than 99% of the time in the intervals  $\pm 90$  and  $\pm 360$  s, respectively. In our numerical study, we assume that IAF time deviations,  $\omega_a$ ,  $a \in \mathcal{A}$ , are identically randomly distributed according to the same normal distribution with mean zero, and given standard deviation  $\sigma$ . Test values for  $\sigma$  are 30, 60, 90, and 120 s.

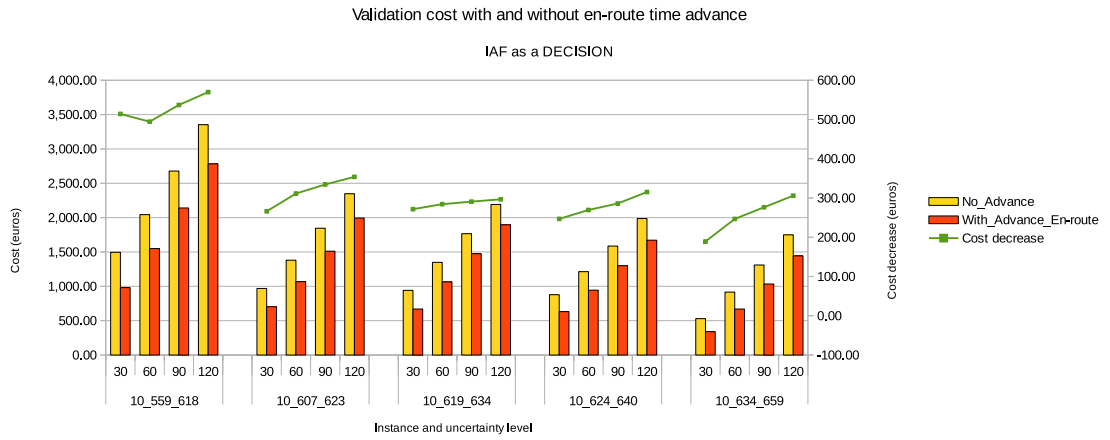
**Delay and advance unit costs.** Unit delay costs by aircraft type, and by flight phase are based on reference values given in Cook and Tanner (2015), a technical report updated in 2015, and more exactly on Tables 26, 28, and 29. We focus on delay lengths of 5, 15, 30, and 60 min to define the abscissa of the breakpoints and the slope of each linear piece. Since the report considers only 15 aircraft types, while in our instances there are 23 aircraft types, we generate reference delay costs, for the eight missing aircraft types, using linear regression, as follows. For the at-gate and en-route phases, coefficients of a linear regression, with the square root of maximum take-off weight, are provided in the report. For the delay cost at the approach phase (called *arrival management* phase in Cook and Tanner (2015)), we found a good linear fit between the unit costs and the number of seats, for each aircraft type. We use the corresponding coefficients to generate the missing unit delay costs at the approach phase.

For the advance cost in the en-route phase, we assume that the unit advance cost is equal to 10% of the fuel-cost portion of the unit delay cost in en-route, for each aircraft type. This assumption is inspired by the numerical study in Lee (2008), and checked directly with the author. Finally, in our data, unit advance cost in en-route represents around 6% of the unit delay cost.

All delay and advance unit costs used in this study are given in Appendix C.



(a) IAF as an input



(b) IAF as a decision

Fig. 6. Decrease in the delay cost when one minute of en-route time advance is allowed,  $d_a^R = 60$  sec, in both problem variants: IAF as an input (a) and IAF as decision (b).

**Number of scenarios.** For all instances, and all uncertainty levels, the number of scenarios for optimization is set to  $n_S = 100$ , and for validation, to  $n_{S'} = 1000$ .

## 6.2. Benefit from en-route time advance

As presented in Section 6.1, this computational study focuses on the case where up to one minute of time advance in the en-route phase is allowed ( $d_a^R = 60$  sec). This main case is called “with advance” case. Only in this subsection, we also study the case where an aircraft cannot be assigned an IAF target time earlier than its planned or unconstrained IAF time (for an airborne or at-gate aircraft, respectively), *i.e.*,  $d_a^R = 0$ ; we refer to this case as the “no advance” case.

Figs. 6(a) and 6(b) depict delay cost decrease for all studied instances and all studied uncertainty levels, due to the one-minute time advance in the en-route phase. The delay cost decrease is computed as the relative difference between the average validation delay costs of stochastic solutions in the “no advance” case and in the “with advance” case. The delay cost decrease, plotted with a green line in both figures, ranges from around 200 euros to more than 550 euros. Hence, allowing time advance helps decreasing significantly the delay cost. This is due to the fact that the unit cost of time advance is very low compared to the unit cost of delay, for all aircraft types, creating thereby a window of opportunity to find lower-cost solutions. This decrease in delay cost comes at the price of longer computing times, with an increase ranging from 2.6 to 46.6 s in the “IAF as an input” variant, and from 4.0 to 344.0 s in the “IAF as a decision” variant. In the remainder of this computational study, we shall only consider the “with advance” case, where  $d_a^R = 60$  s (see Fig. 6).



**Table 9**

Result summary of the stochastic solutions of all instances for the case “IAF as a decision” with en-route advance.

Instance	$\sigma$	CPU	Validation score	VSS		Avg nb IAF changes	# diff seq		
				euros	%		IAF 1	IAF 2	RWY
10_559_618	30	50.03	980.75	-117.36	-10.69%	1.0	1	1	1
	60	116.07	1,549.53	-219.65	-12.42%	1.9	2	2	2
	90	157.68	2,141.14	-347.28	-13.96%	2.9	2	2	1
	120	165.92	2,783.25	-477.72	-14.65%	3.0	1	1	1
10_607_623	30	55.21	702.86	-166.68	-19.17%	0.0	1	1	1
	60	65.05	1,068.42	-297.77	-21.80%	0.0	1	1	1
	90	79.24	1,511.39	-376.39	-19.94%	0.6	2	2	2
	120	91.80	1,994.27	-451.53	-18.46%	0.9	3	3	4
10_619_634	30	82.39	669.42	-17.42	-2.54%	0.0	1	1	1
	60	140.28	1,064.62	-19.70	-1.82%	0.0	2	2	3
	90	482.67	1,475.07	-31.35	-2.08%	0.0	2	2	5
	120	608.00	1,895.56	-63.15	-3.22%	0.0	2	2	3
10_624_640	30	326.57	631.36	-86.75	-12.08%	0.0	1	1	1
	60	530.76	943.70	-136.85	-12.66%	0.1	2	2	1
	90	566.34	1,299.71	-166.19	-11.34%	0.9	5	3	6
	120	538.87	1,671.35	-208.38	-11.09%	1.4	4	4	5
10_634_659	30	9.80	340.64	-55.46	-14.00%	0.0	1	2	2
	60	33.82	669.45	-109.40	-14.05%	0.5	2	2	2
	90	73.97	1,033.71	-189.99	-15.53%	1.0	1	2	2
	120	137.94	1,443.08	-268.70	-15.70%	1.0	1	2	2

### 6.3. Summary results

Summary results of the stochastic solutions for the two variants (“IAF as a decision” and “IAF as an input”) are given in [Tables 9](#) and [10](#). “CPU” stands for the computing time, expressed in seconds, as returned by CPLEX, of stochastic solutions, averaged over  $n_R = 10$  replications. The “Validation score” column reports the average validation score of stochastic solutions obtained for  $n_R = 10$  replications, which gives an order of magnitude of the time-deviation cost (in euros) for each test setup. The “VSS” column displays the value of the stochastic solution. Definitions of validation score and VSS of a stochastic solution, are given in [Section 5.2](#). The number of IAF changes averaged over 10 replications is given (only in [Table 9](#)) in column “Avg nb IAF changes”. The last three columns “# diff seq IAF 1”, “IAF 2”, and “RWY” give the number of unique IAF 1, IAF 2, and runway sequences, given that 10 replications of each problem are solved. A low number of unique sequences shows that there is low discrepancy among different replications. Ideally, when for a given test setup (an instance, and an uncertainty level), stochastic solutions from all replications are identical (or at least, the solution sequences are identical), this indicates that solving only one replication suffices, and that the number of second-stage scenarios,  $n_S$ , is sufficiently large to capture the information behind the original complete set of scenarios.

### 6.4. Value of the stochastic solution

For all instances and all uncertainty levels, VSS, given in [Tables 9](#) and [10](#), is negative and decreases as uncertainty level increases. Negative VSS shows that stochastic solutions perform better than deterministic solutions, in terms of time-deviation costs, when all solutions are evaluated on the same large uncertainty-scenario set. The cost saving of stochastic solutions compared to their deterministic counterparts, for the very high uncertainty level ( $\sigma = 120$  s), as given by the relative VSS, ranges from 3.22% to 18.46% less than the time-deviation cost of deterministic solutions (corresponding to 63.15 euros and to 451.53 euros respectively). This illustrates that there is a significant benefit from taking into account uncertainty through two-stage stochastic programming, and that this benefit is more prominent for higher levels of uncertainty, as expected.

We observe that the VSS in the “IAF as a decision” and the “IAF as an input” variants are very similar, for all instances, except for instance 10\_559\_618. In fact, stochastic solutions from both variants are quite similar, and the average number of IAF changes is low, except for instance 10\_559\_618 whose stochastic solution features 3 IAF changes. This suggests that flexible IAF assignment can be used to mitigate uncertainty.

#### Comparison of the deterministic and the stochastic solutions

In order to understand better the reason behind large VSS, for uncertainty level  $\sigma = 120$  s, we plot in [Figs. 7](#) and [8](#) the breakdown of validation costs and of delay and advance times, for each problem variant. Very importantly, these figures highlight the difference in cost and time (delay and advance) between deterministic and stochastic solutions, at each flight phase: at-gate, en-route, and approach phases.

**Table 10**

Result summary of the stochastic solutions of all instances for the case “IAF as an input” with en-route advance.

Instance	$\sigma$	CPU	Validation score	VSS		# diff seq		
				euros	%	IAF 1	IAF 2	RWY
10_559_618	30	26.42	994.72	-103.39	-9.42%	1	1	1
	60	49.63	1,614.05	-155.13	-8.77%	1	2	2
	90	62.73	2,217.15	-271.27	-10.90%	1	1	1
	120	82.39	2,890.82	-370.16	-11.35%	1	1	1
10_607_623	30	26.23	702.86	-166.68	-19.17%	1	1	1
	60	33.02	1,068.42	-297.77	-21.80%	1	1	1
	90	40.99	1,512.11	-375.68	-19.90%	1	1	1
	120	42.51	2,010.65	-435.14	-17.79%	1	3	3
10_619_634	30	38.46	669.42	-17.42	-2.54%	1	1	1
	60	58.86	1,064.62	-19.70	-1.82%	2	2	3
	90	90.63	1,475.07	-31.35	-2.08%	2	2	5
	120	114.42	1,895.56	-63.15	-3.22%	2	2	3
10_624_640	30	65.94	631.36	-86.75	-12.08%	1	1	1
	60	107.83	943.55	-136.99	-12.68%	1	1	1
	90	106.68	1,300.87	-165.03	-11.26%	3	1	4
	120	109.42	1,680.39	-199.33	-10.60%	2	2	6
10_634_659	30	5.57	340.64	-55.46	-14.00%	1	2	2
	60	12.93	672.04	-106.82	-13.71%	1	1	1
	90	24.94	1,069.60	-154.10	-12.59%	2	2	3
	120	37.97	1,481.62	-230.16	-13.45%	2	3	4

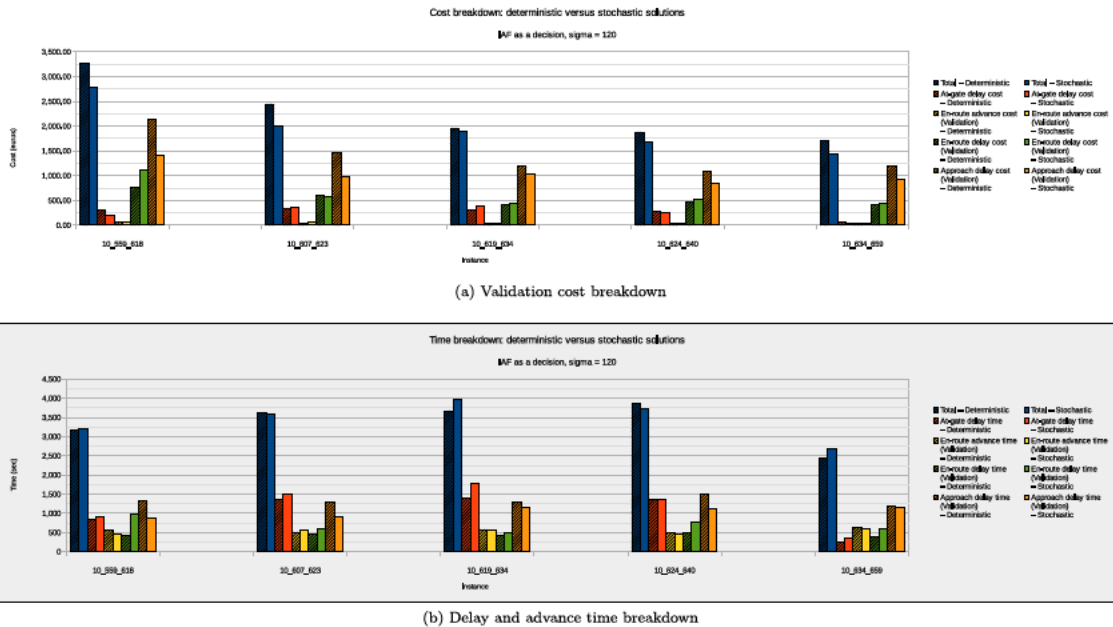


Fig. 7. Validation cost and time breakdown, by flight phase, of the deterministic and the stochastic solutions, of the “IAF as a decision” problem variant.

Most of the benefit of the stochastic solutions when IAF assignment is fixed comes from smaller delays in the approach phase, at the expense of larger delays at gate. In fact, since delay cost is much lower at gate than in other flight phases, there is a significant saving in the approach delay cost, while the additional cost in the at-gate phase is negligible.

The same remark holds also for the problem where IAF assignment is flexible. However, in this latter variant, an additional remark is that, in the stochastic solutions, there is often an increase in both delay cost and delay time in the en-route phase. This is due to IAF changes occurring in some stochastic solutions (as shown in Table 9), and not in the deterministic solutions, of the studied instances. Recall that every IAF change induces 5 min of additional delay in the en-route phase.

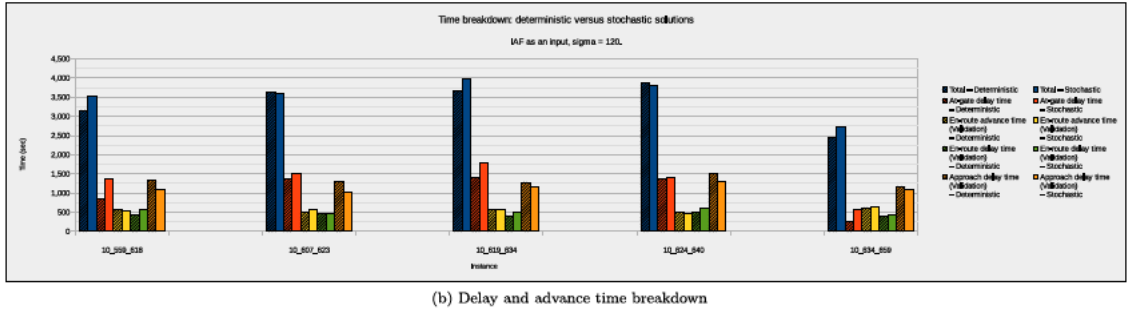
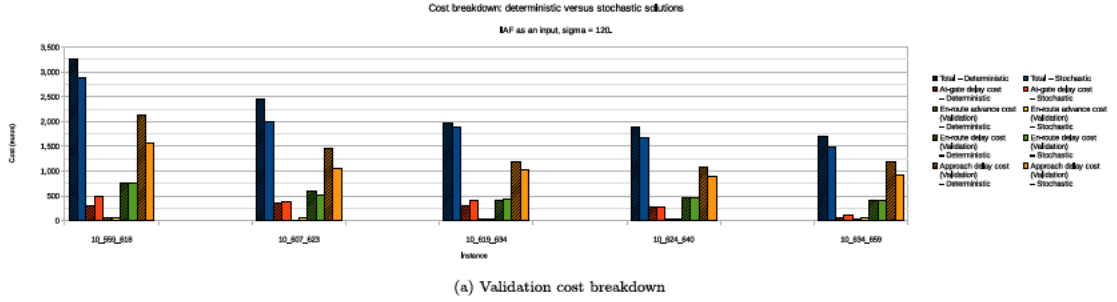


Fig. 8. Validation cost and time breakdown, by flight phase, of the deterministic and the stochastic solutions, of the “IAF as an input” problem variant.

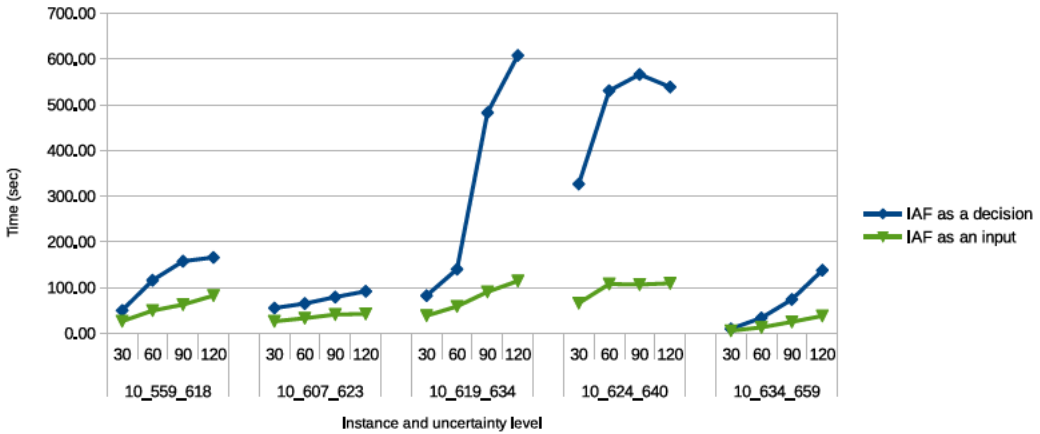


Fig. 9. Average computation time for all instances and uncertainty levels in the “IAF as a decision” and the “IAF as an input” problem variants.

### 6.5. Effect of flexible IAF assignment

This subsection discusses the effect of the additional degree of freedom of re-assigning IAFs to flights, two to three hours before landing. The “IAF as decision” variant requires more computation time than the “IAF as input” variant, as shown in Fig. 9. This is explained by the additional decision to make, and hence the larger solution space. Instances 10\_619\_634 and 10\_624\_640 show a significant difference in CPU time between both problem variants, especially for large uncertainty levels ( $\sigma = 90, 120$  s). It is noteworthy that these two instances are the most compressed ones, *i.e.*, those having the shortest time spans (difference between the last and the first planned landings), as given in Table 6.

Fig. 10 displays the validation costs for all instances and all uncertainty levels for both problem variants, as well as the cost saving obtained from allowing flexible IAF assignment. The cost saving, plotted as “(Pos) Cost saving” in Fig. 10, is defined as the difference between the validation costs of both problem variants:

$$\text{Cost saving} = \text{Validation cost(IAF as an input)} - \text{Validation cost(IAF as a decision)}$$

Through all test setups, the cost saving ranges from zero to 107.56 euros, showing that for some instances re-assigning IAFs to flights can help to reduce delay and advance costs. Fig. 11 reveals a correlation between the cost saving and the average number

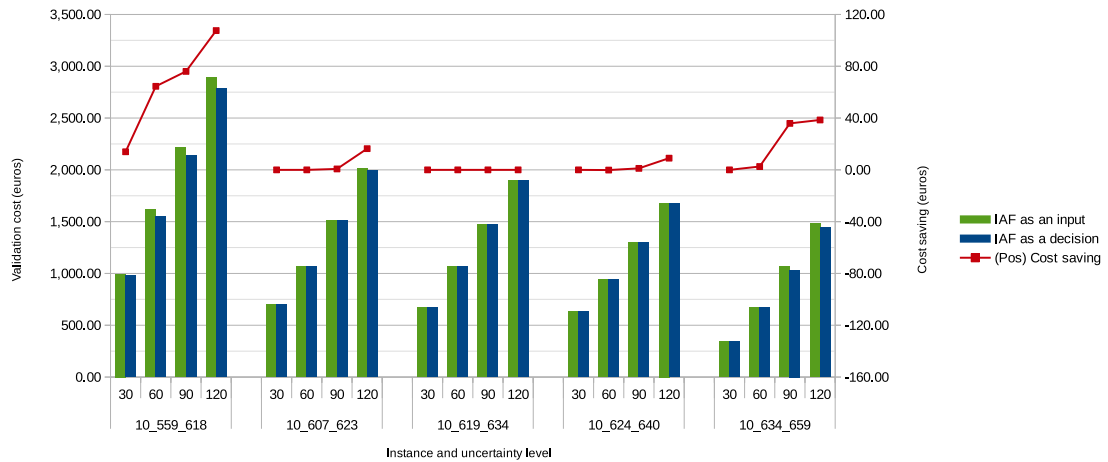


Fig. 10. Validation costs for all instances and uncertainty levels in the “IAF as a decision” and the “IAF as an input” problem variants. Positive cost saving is the gain from flexible IAF assignment.

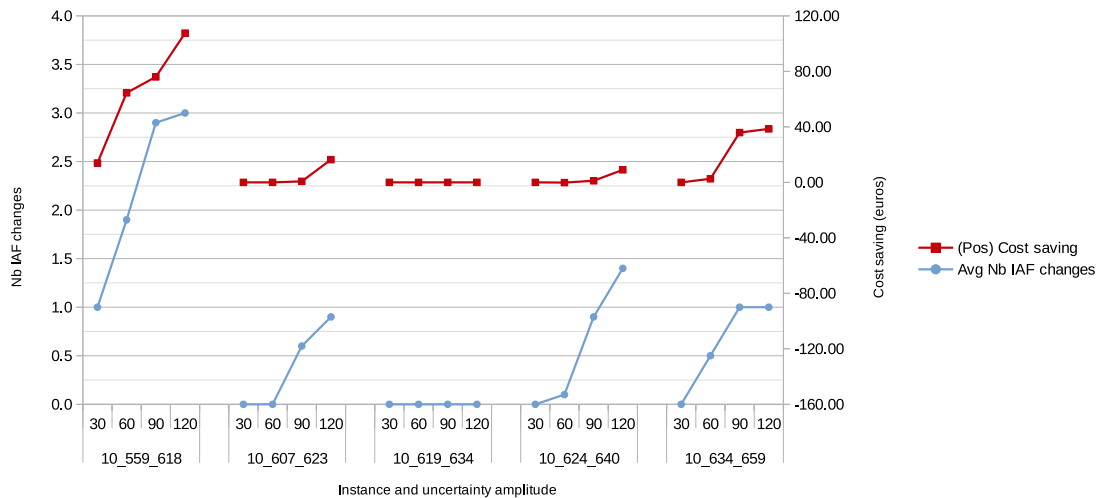


Fig. 11. Relationship between cost saving due to flexible IAF assignment and average number of IAF changes, for all instances and uncertainty levels.

of IAF changes. When there is no IAF change in the stochastic solutions of the “IAF as a decision” problem variant (as in instance 10\_619\_634), there is no cost saving compared to the variant “IAF as an input”; in such a test setup, solutions from both variants are identical (yet, more CPU time is needed to find them in the “IAF as a decision” variant). On the other hand, more IAF changes induce more cost saving, as illustrated clearly in instance 10\_559\_618, for example. We also see that the average number of IAF changes increases, as uncertainty increases, for most instances (all instances but 10\_619\_634). Hence, flexible IAF change can act as a hedging measure against uncertainty.

For a more thorough understanding of the added value of stochastic solutions compared to deterministic ones, and of the benefit of flexible against fixed IAF assignment, we focus in the next subsection on the test setup involving the largest VSS, and the largest average number of IAF changes in the stochastic solutions: instance 10\_559\_618 with uncertainty level  $\sigma = 120$  s.

#### 6.6. Detailed results of a typical instance with high VSS and high cost saving due to IAF change

According to Tables 9 and 10, instance 10\_559\_618, together with uncertainty level  $\sigma = 120$  s, features the largest value of the stochastic solution ( $-477.72$  and  $-370.16$  euros, for the “IAF as a decision” and “IAF as an input” problem variants, respectively), as well as the largest number of IAF changes (3 flights change their IAF). Table 11 describes this instance in more detail.

As a preliminary remark, the deterministic solutions for this test setup are identical for both problem variants. For the stochastic solution of each problem variant, we select the one with the smallest validation cost among the solutions of the  $n_R = 10$  replications that we solved. We call such a solution the “best” stochastic solution for the considered problem variant. In this subsection, we

**Table 11**

Instance 10\_559\_618 with, for each flight: the flight status (2-3 h before landing), the aircraft type, the wake turbulence category (WTC), the initial IAF, the planned departure, and the planned landing times.

Id	Callsign	Flight status	Aircraft type	WTC	Initial IAF	Planned departure	Max at-gate delay	Planned landing
1	NLY966D	On-ground	A320	M	2	346	900	7846
2	AFR007	Airborne	A388	H	1	NA	0	7920
3	GW16Z	On-ground	A319	M	2	3451	900	7951
4	AFR379	Airborne	B772	H	1	NA	0	8096
5	AFR347	Airborne	A343	H	1	NA	0	8124
6	GW198M	On-ground	A320	M	2	2086	900	8086
7	DAL400	Airborne	A333	H	1	NA	0	8232
8	UAL904	Airborne	B763	H	1	NA	0	8280
9	DLH68H	On-ground	E190	M	2	2602	900	8302
10	AFR639	Airborne	B77W	H	1	NA	0	8476
COUNT		(6) Airborne (4) On-ground		(4) M (6) H	(6) IAF 1 (4) IAF 2			

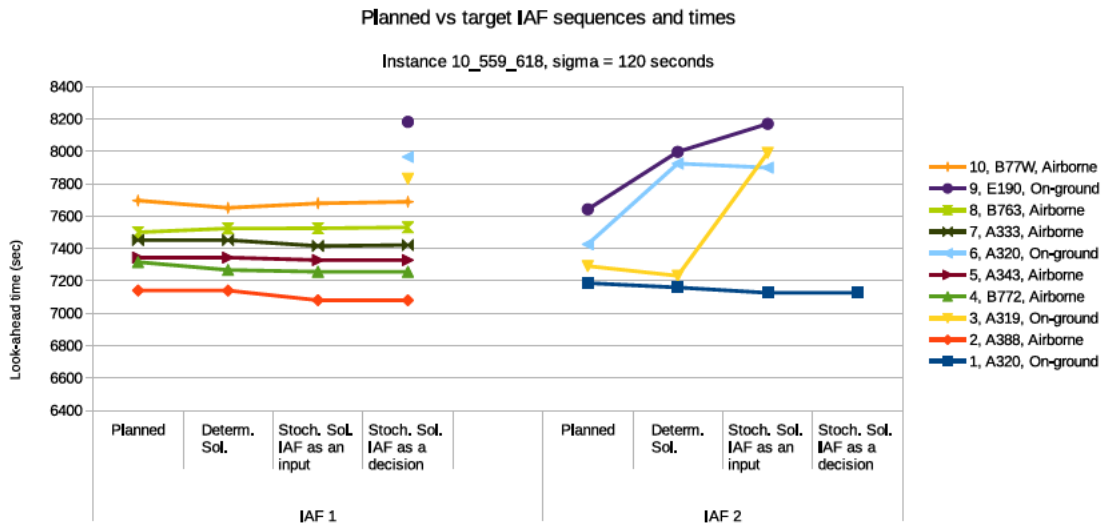


Fig. 12. Planned, target IAF sequences, and target IAF times for all three solutions, of instance 10\_559\_618, and  $\sigma = 120$  s.

compare three solutions: the deterministic solution, the “best” stochastic solution of the “IAF as an input” problem variant, and the “best” stochastic solution of the “IAF as a decision” problem variant.

Target IAF sequences as well as target IAF times for all three solutions are illustrated in Fig. 12. The y-axis represents target IAF times, cast as look-ahead times to IAF in seconds. For example, the value 7200 corresponds to an aircraft that should arrive at IAF in exactly 2 h, from the decision time. That is: if we are making first-stage decisions at 08:00 in the morning, then this aircraft’s target IAF time is 10:00. The x-axis is mainly divided into two parts. The left-hand part displays sequences for IAF 1, and the right-hand part displays those for IAF 2. For each IAF, we plot four sequences: “Planned” (based on planned IAF times), “Determ. Sol.” (based on target IAF times from the retained deterministic solution), “Stoch. Sol. IAF as an input” (based on target IAF times from the retained stochastic solution when IAF assignment is an input), and “Stoch. Sol. IAF as a decision” (based on target IAF times from the retained stochastic solution when IAF assignment is a decision). Every aircraft is distinguished by a unique color and a unique label across all sequences of both IAFs. Moreover, the positions of each aircraft, in every two consecutively-plotted sequences for the same IAF, are linked with a straight line. We note that in all solutions, target IAF sequences conserve the first-come, first-serve order, except for a single overtaking occurring in IAF-2 sequence of the stochastic solution, when IAF assignment is considered as an input. We observe that aircraft 6, and 9 are sharply delayed, with respect to their planned IAF time, in all three solutions. Aircraft 3 is also much delayed in both stochastic solutions. Finally, aircraft 3, 6, and 9 are rerouted to an IAF different from their initial one, in the stochastic solution, when IAF assignment is flexible.

Validation costs, and delay and advance times, by flight phase, for the three solutions are illustrated in Figs. 13(a) and 13(b). We remark that delay time in at-gate and en-route phases are smaller in the deterministic solution, than in the two stochastic solutions, while delay in the approach phase is higher. On the other hand, from the total time-deviation cost perspective (which is the quantity that the model minimizes), both stochastic solutions perform better than the deterministic solution. Let us recall that the unit cost of delay in approach is usually much higher than in the two other flight phases. For this reason, stochastic solutions hedge against

uncertainty by avoiding delay in the approach phase, and by applying, instead, larger delays in the upstream phases, than in the deterministic solution. In fact, the deterministic solution considers only one second-stage scenario, where all aircraft arrive at IAF on time (*i.e.*, the *mean* scenario). When confronted with scenarios having large uncertainties, the delays to apply in the approach phase, assuming the first-stage decision is the deterministic solution, are large and their cost is large too. This inverted tendency between minimization of delay time and minimization of delay cost, has also been observed in the literature, yet in a different deterministic optimization problem for air traffic flow management (Bolić et al., 2017), where similar unit delay cost from Cook and Tanner (2015) are used.

From the distribution of cost and time over the flight phases (Figs. 13(a) and 13(b)), we deduce that the stochastic solution, when IAF assignment is fixed, uses as much as possible the delay at gate, since it is less expensive than in other flight phases. This is to anticipate as much as possible the delay to be encountered in the approach phase, where delay unit cost becomes very high. In an analogous way, the stochastic solution, when IAF re-assignment is possible, anticipates again delay in the approach phase, by rerouting three flights to a different IAF. More precisely, these three aircraft are asked to change their IAF from IAF 2, the IAF closest to the runway threshold, to IAF 1, that is the farthest IAF away from the runway threshold. These reroutings have two direct effects. Firstly, they increase delay time and cost in the en-route phase, compared to the other two solutions. Secondly, they defer the unconstrained landing times of the three rerouted aircraft, used to compute delay at approach. This is particularly convenient and cost efficient for these three aircraft since they are computed as the last three aircraft to land according to the target landing sequence, as shown in Fig. 14. With later unconstrained landing times, the three rerouted aircraft will need less delay (and less cost) in the approach phase, in order to achieve their target positions in the landing sequence.

The breakdown of the validation results (cost and time) by flight phase and by aircraft, shown in Figs. 15(a) to 15(h), confirms the last remark. Moreover, we observe that aircraft 2 (an A388, already airborne at the beginning of the optimization) has a huge delay cost in the approach phase, in the deterministic solution, where this aircraft is computed to land in the third position after an A319 (see Fig. 14). In fact, A388 has the largest delay unit cost, particularly in the approach phase, among all considered aircraft types. According to the landing sequence of the deterministic solution, the first aircraft (an A320) can land without delay, *i.e.*, exactly at its unconstrained landing time. Then, the A319 can land soon after that A320 aircraft, by leaving the required runway threshold separation (but also never before its own unconstrained landing time). For the third position, the A388 has to be separated from the A319. Note that if in any scenario, the A319 has to be delayed for separation with the A320, and that such a delay consumes the buffer between the A319 and the A388, then the A388 will have to be further delayed in order to be separated from the A319. However, the two stochastic solutions decided to delay the A319 towards the end of sequence, so that the A388 can land in the second position without being affected by the possible delay incurred by the A319. This is also motivated by the fact that an A319 has relatively low delay unit costs.

In the stochastic solution when IAF assignment is fixed, the A319 is delayed on the ground by more than 10 min. In this case, the cost of at-gate delay covers entirely the first piece of the piecewise-defined cost function, from 0 to 5 min, and partially the second piece, from 5 to 15 min. Recall that the delay unit cost of the second piece is higher than that of the first piece, as the delay cost function is convex. In the stochastic solution when IAF assignment is flexible, the A319 is delayed at gate by 5 min exactly. In the en-route phase, it is rerouted to a different IAF, causing 5 min of delay, and expedited by one minute; overall it is delayed by around 4 min. However, the validation delay time is computed after uncertainty is revealed. Thus, for a given uncertainty scenario, the validation delay time for the A319 in the en-route phase can be less or greater than 4 min, depending on the uncertainty amount. The validation delay time for the A319 in the en-route phase, averaged over all validation scenarios, is around 250 s. Similar observations can be made for aircraft 6 (A320), and 9 (E190). Remark also that the validation delay and advance cost for all three rerouted aircraft (in the stochastic solution when IAF assignment is flexible) are smaller than in the stochastic solution when IAF assignment is fixed. This confirms that IAF re-assignment, modeled as a path stretching in the en-route phase, can be an efficient measure to decrease overall delay cost in the extended arrival management context (see Fig. 13).

## 7. Conclusions and perspectives

We build on the literature of the extended aircraft arrival management problem under uncertainty (Khassiba et al., 2019, 2020) by proposing a two-stage stochastic programming formulation that takes into account three new operational aspects: (i) multiple IAFs feeding the landing runway, (ii) different flight status in the first stage (aircraft are initially either at departure gate or airborne), and (iii) a time-deviation-cost function to minimize that is based on reference values depending on aircraft type and flight phase, based on Cook and Tanner (2015). We formulate and study two problem variants. The first variant considers the general case of flexible re-assignment of IAFs to aircraft, as a new decision in the first stage. In the second variant, IAF assignment is assumed to be given as an input and fixed.

We conduct a computational study on five realistic instances from Paris Charles-de-Gaulle airport, each of which involves 10 aircraft and two IAFs. For large uncertainty, values of the stochastic solution show a decrease in the time-deviation cost ranging from 3.22% to 18.46% of the deterministic solutions' cost. This illustrates the benefit of taking into account uncertainty through two-stage stochastic programming. As for the effect of flexible IAF assignment, through the detailed study of a typical instance, we remark that IAF changes help to decrease time-deviation cost, showing that IAF re-assignment can act as a hedging measure against uncertainty.

An even more realistic study would take into account not only uncertainty but also the dynamic nature of the operational problem: continuously, new aircraft enter, while other aircraft leave the optimization horizon. Very recently, a few works tackled the problem of aircraft scheduling and sequencing in the dynamic context, taking into account uncertainty (Huo et al., 2021; Vié et al., 2022). Perspectives of the current work include extending the two-stage stochastic programming formulation to the dynamic case. Similar approaches have already been applied to other scheduling problems in transportation (see *e.g.*, Zhu and Goverde (2020)). Advanced solution methods, *e.g.*, based on Benders decomposition, may also be explored to reduce the computation time.

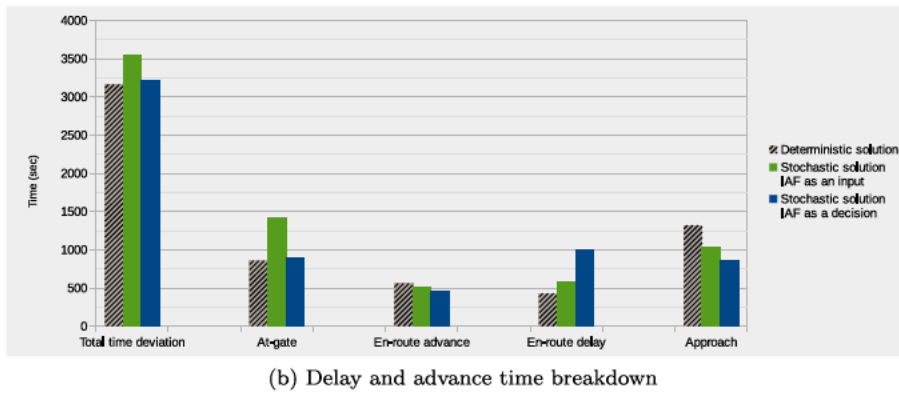
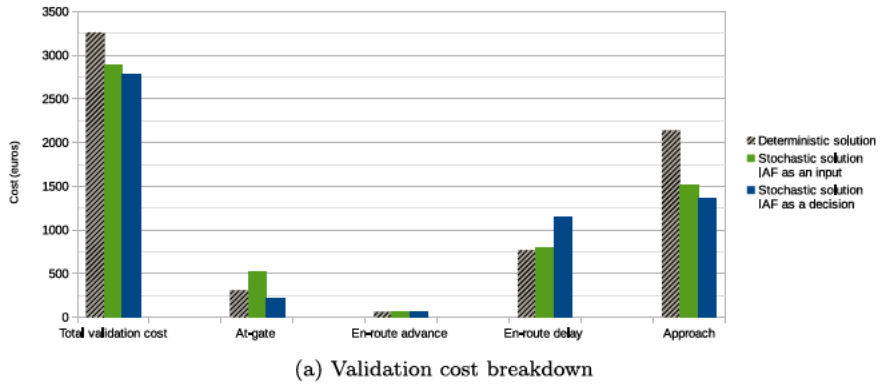


Fig. 13. Validation cost and time breakdown, by flight phase, of the deterministic, the stochastic solutions when IAF assignment is an input, and when it is a decision, for instance 10\_559\_618, and uncertainty level  $\sigma = 120$  s.

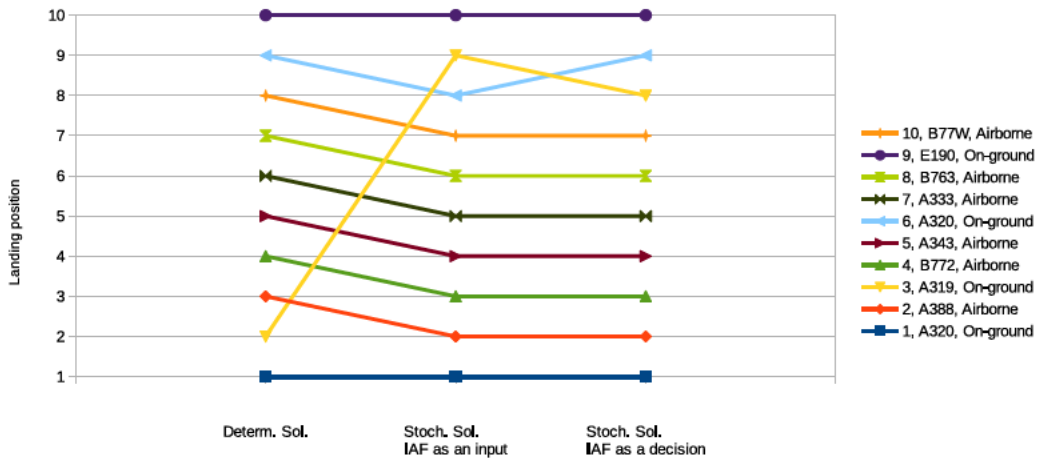
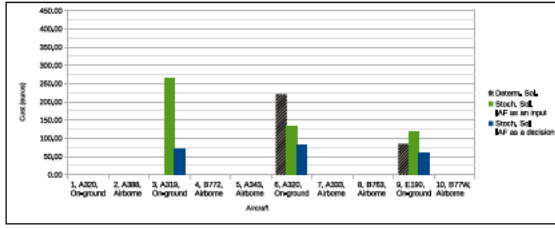


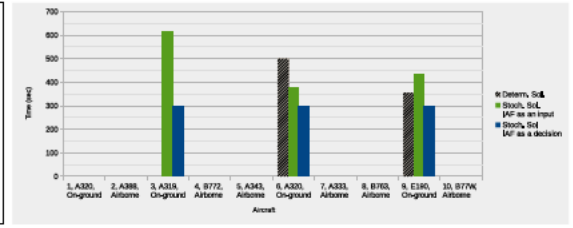
Fig. 14. Target landing sequences, for all three solutions, of instance 10\_559\_618, and  $\sigma = 120$  s.

### CRediT authorship contribution statement

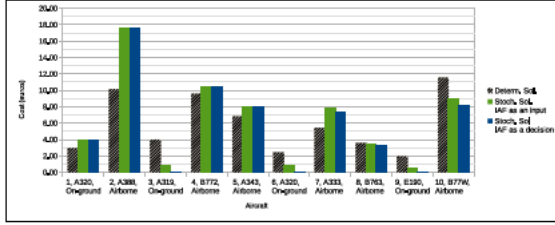
**Ahmed Khassiba:** Conceptualization, Methodology, Software, Writing – original draft. **Sonia Cafieri:** Supervision, Conceptualization, Writing – review & editing. **Fabian Bastin:** Supervision, Conceptualization, Writing – review & editing, Funding acquisition. **Marcel Mongeau:** Supervision, Validation, Writing – review & editing. **Bernard Gendron:** Supervision, Writing – review & editing, Funding acquisition.



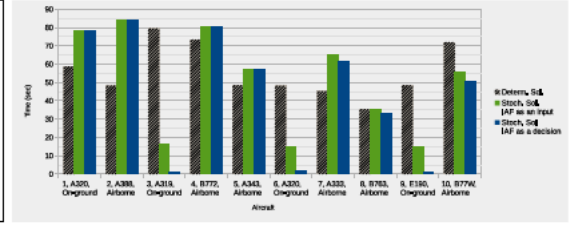
(a) At-gate validation delay cost breakdown



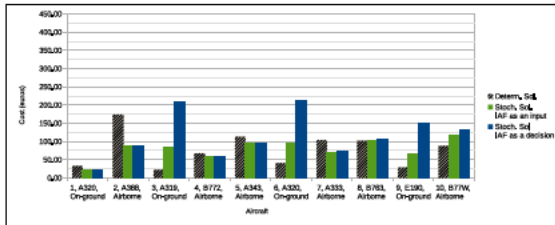
(b) At-gate delay time breakdown



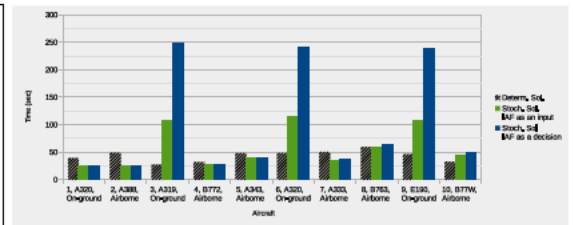
(c) En-route validation advance cost breakdown



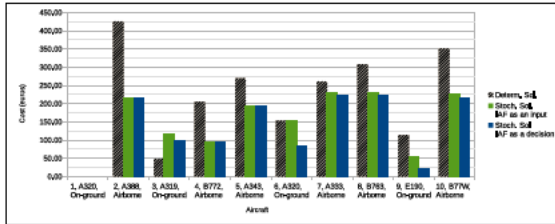
(d) En-route advance time breakdown



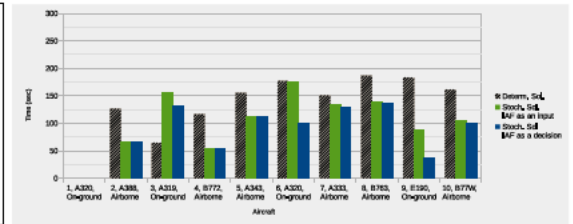
(e) En-route validation delay cost breakdown



(f) En-route delay time breakdown



(g) Approach validation delay cost breakdown



(h) Approach delay time breakdown

Fig. 15. Validation cost and time breakdown, by flight phase, and by aircraft, of the deterministic, the stochastic solutions when IAF assignment is an input, and when it is a decision, for instance 10\_559\_618, and uncertainty level  $\sigma = 120$  s.

## Acknowledgments

The work of Fabian Bastin and Bernard Gendron is supported by the Natural Sciences and Engineering Research Council of Canada. [Discovery Grants 2017-05798 and 2017-06054 respectively].

## Appendix A. Expressions of best bounds on target IAF time and target landing time

### A.1. First-variant model: IAF as a first-stage decision

#### A.1.1. Expressions of best bounds on target IAF time: $E_b^{best}$ and $L_a^{best}$

See Table A.1.

### Proofs

- Expression of  $E_b^{best}$



**Table A.1**

Expressions of the constants  $E_b^{\text{best}}$  and  $L_a^{\text{best}}$  that occur in the definition of the big-M constant  $M_{ab}$  according to flight status (case where IAF assignment is a first-stage decision). Same as Table 3.

Flight status	On-ground (in $\mathcal{A}^G$ )	Airborne (in $\mathcal{A}^A$ )
$E_b^{\text{best}}$	$P_b^{\text{TOT}} + \hat{V}_b^O - \underline{d}_b^R$	$E_b^{j^*}$ , where $j^*$ is the initial IAF of $b$
$L_a^{\text{best}}$	$P_a^{\text{TOT}} + \bar{d}_a^G + \hat{V}_a^O + r + \bar{d}_a^R$	$L_a^k$ , where $k \in \mathcal{I} \setminus \{i^*\}$ is an IAF <i>different</i> from $i^*$ the initial IAF of $a$

**Table A.2**

Expressions of the constants  $E_b^{L,\text{best}}$  and  $L_a^{L,\text{best}}$  that occur in the definition of the big-M constant  $M_{ab}^L$  according to flight status (case where IAF assignment is a first-stage decision). Same as Table 4.

Flight status	On-ground (in $\mathcal{A}^G$ )	Airborne (in $\mathcal{A}^A$ )
$E_b^{L,\text{best}}$	$P_b^{\text{TOT}} + \hat{V}_b^O - \underline{d}_b^R + \omega_b + \min_{k \in \mathcal{I}} \{ \underline{V}_b^k + r^{j^*k} \}$ where $j^* \in \mathcal{I}$ is the initial IAF of aircraft $b$	$P_b^{j^*} - \underline{d}_b^R + \omega_b + \min_{k \in \mathcal{I}} \{ \underline{V}_b^k + r^{j^*k} \}$
$L_a^{L,\text{best}}$	$P_a^{\text{TOT}} + \bar{d}_a^G + \hat{V}_a^O + \bar{d}_a^R + \omega_a + \max_{k \in \mathcal{I}} \{ \bar{V}_a^k + r^{i^*k} \}$ where $i^* \in \mathcal{I}$ is the initial IAF of aircraft $a$	$P_a^{i^*} + \bar{d}_a^R + \omega_a + \max_{k \in \mathcal{I}} \{ \bar{V}_a^k + r^{i^*k} \}$

- For an on-ground aircraft  $b \in \mathcal{A}^G$ , with an initial IAF  $j^* \in \mathcal{I}$ , and assigned IAF  $k \in \mathcal{I}$ , we have:

$$x_b \geq t_a + \hat{V}_a^O + r^{j^*k} - \underline{d}_b^R \geq P_a^{\text{TOT}} + \hat{V}_a^O - \underline{d}_b^R \tag{A.1}$$

- For an airborne aircraft  $b \in \mathcal{A}^A$ : the expression of the smallest earliest IAF time is trivial, since any rerouting will cause a delay in the en-route phase. Hence, for any IAF different from the initial IAF, the earliest IAF time is greater than the earliest IAF time for the initial IAF. We obtain:

$$x_b \geq E_b^k = E_b^{j^*} + r^{j^*k} \geq E_b^{j^*} \tag{A.2}$$

- Expression of  $L_a^{\text{best}}$

- For an on-ground aircraft  $a \in \mathcal{A}^G$ , with an initial IAF  $j^* \in \mathcal{I}$ , and assigned IAF  $k \in \mathcal{I}$ , we have:

$$x_a \leq t_a + \hat{V}_a^O + r^{j^*k} + \bar{d}_b^R \leq P_a^{\text{TOT}} + \bar{d}_a^G + \hat{V}_a^O + r + \bar{d}_a^R \tag{A.3}$$

- For an airborne aircraft  $a \in \mathcal{A}^A$ : the expression of the greatest latest IAF time is trivial, since any rerouting will cause a delay in the en-route phase. Hence, for any IAF different from the initial IAF, the latest IAF time is greater than the latest IAF time for the initial IAF, by  $r$  seconds:

$$x_a \leq L_a^k = L_a^{i^*} + r^{i^*k} \tag{A.4}$$

$$\max_{k \in \mathcal{I}} \{ L_a^k \} = L_a^{i^*} + r \tag{A.5}$$

### A.1.2. Expressions of best bounds on target landing time: $E_b^{L,\text{best}}$ and $L_a^{L,\text{best}}$

See Table A.2.

#### Proofs

- Expression of  $E_b^{L,\text{best}}$

- For an on-ground aircraft  $b \in \mathcal{A}^G$ , assigned to IAF  $k \in \mathcal{I}$ , we have:

$$y_b \geq x_b + \omega_b + \underline{V}_b^k \tag{A.6}$$

$$\geq P_b^{\text{TOT}} + \hat{V}_b^O + r^{j^*k} - \underline{d}_b^R + \omega_b + \underline{V}_b^k \tag{A.7}$$

Given that IAF  $k$  is unknown before optimization, we can write:

$$E_b^{L,\text{best}} = \min_{k \in \mathcal{I}} \{ P_b^{\text{TOT}} + \hat{V}_b^O - \underline{d}_b^R + \omega_b + \underline{V}_b^k + r^{j^*k} \} \tag{A.8}$$

$$= P_b^{\text{TOT}} + \hat{V}_b^O - \underline{d}_b^R + \omega_b + \min_{k \in \mathcal{I}} \{ \underline{V}_b^k + r^{j^*k} \} \tag{A.9}$$

**Table A.3**

Expressions of the constants  $E_b^{\text{best}}$  and  $L_a^{\text{best}}$  that occur in the expression of the big-M constant  $M_{ab}^L$  according to flight status (case where IAF assignment is fixed). Same as Table 5.

Flight status	On-ground (in $\mathcal{A}^G$ )	Airborne (in $\mathcal{A}^A$ )
$E_b^{\text{best}}$	$P_b^{\text{TOT}} + \hat{V}_b^O - \underline{d}_b^R$	$E_b^{i^*}$ (input data)
$L_a^{\text{best}}$	$P_a^{\text{TOT}} + \bar{d}_a^G + \hat{V}_a^O + \bar{d}_a^R$	$L_a^{i^*}$ (input data)

– For an airborne aircraft  $b \in \mathcal{A}^A$ , assigned to IAF  $k \in I$ , we have:

$$y_b \geq x_b + \omega_b + \underline{V}_b^k \tag{A.10}$$

$$\geq P_b^{i^*} + r^{i^*k} - \underline{d}_b + \omega_b + \underline{V}_b^k \tag{A.11}$$

Given that IAF  $k$  is unknown before optimization, it follows:

$$E_b^{L,\text{best}} = \min_{k \in I} \left\{ P_b^{i^*} + r^{i^*k} - \underline{d}_b + \omega_b + \underline{V}_b^k \right\} \tag{A.12}$$

$$= P_b^{i^*} - \underline{d}_b + \omega_b + \min_{k \in I} \left\{ \underline{V}_b^k + r^{i^*k} \right\} \tag{A.13}$$

• Expression of  $L_a^{L,\text{best}}$

– For an on-ground aircraft  $a \in \mathcal{A}^G$ , we have:

$$y_a \leq x_a + \omega_a + \bar{V}_a^k + \bar{d}_a^R \tag{A.14}$$

$$\leq \left( P_a^{\text{TOT}} + \bar{d}_a^G + \hat{V}_a^O + r^{i^*k} \right) + \omega_a + \bar{V}_a^k + \bar{d}_a^R \tag{A.15}$$

Given that the assigned IAF  $k$  is unknown before optimization, we can write:

$$L_a^{L,\text{best}} = \max_{k \in I} \left\{ P_a^{\text{TOT}} + \bar{d}_a^G + \hat{V}_a^O + r^{i^*k} + \omega_a + \bar{V}_a^k + \bar{d}_a^R \right\} \tag{A.16}$$

$$= P_a^{\text{TOT}} + \bar{d}_a^G + \hat{V}_a^O + \bar{d}_a^R + \omega_a + \max_{k \in I} \left\{ \bar{V}_a^k + r^{i^*k} \right\} \tag{A.17}$$

– For an airborne aircraft  $a \in \mathcal{A}^A$ , assigned to IAF  $k \in I$ , we have:

$$y_a \leq x_a + \omega_a + \bar{V}_a^k \leq P_a^{i^*} + r^{i^*k} + \omega_a + \bar{V}_a^k + \bar{d}_a^R \tag{A.18}$$

Given that the assigned IAF  $k$  is unknown before optimization, we obtain:

$$L_a^{L,\text{best}} = \max_{k \in I} \left\{ P_a^{i^*} + r^{i^*k} + \omega_a + \bar{V}_a^k + \bar{d}_a^R \right\} \tag{A.19}$$

$$= P_a^{i^*} + \omega_a + \bar{d}_a^R + \max_{k \in I} \left\{ \bar{V}_a^k + r^{i^*k} \right\} \tag{A.20}$$

## A.2. Second-variant model: IAF as a problem input

See Table A.3.

### A.2.1. Expressions of best bounds on target IAF time: $E_b^{\text{best}}$ and $L_a^{\text{best}}$

Proofs

• The expression of  $E_b^{\text{best}}$  for an on-ground aircraft  $b \in \mathcal{A}^G$  comes from:

$$x_b \geq t_a + \hat{V}_a^O - \underline{d}_b^R \geq P_a^{\text{TOT}} + \hat{V}_a^O - \underline{d}_b^R \tag{A.21}$$

• The expression of  $L_a^{\text{best}}$  for an on-ground aircraft  $a \in \mathcal{A}^G$  comes from:

$$x_a \leq t_a + \hat{V}_a^O + \bar{d}_b^R \leq P_a^{\text{TOT}} + \bar{d}_a^G + \hat{V}_a^O + \bar{d}_b^R \tag{A.22}$$

## Appendix B. Instances

See Table B.1.

## Appendix C. Delay and advance unit costs

See Table C.1

**Table B.1**

Original instance of 30 aircraft with initial IAFs and flight status. (559\_659)

Callsign	Flight status	Aircraft type	WTC	Initial IAF	At-gate		Planned landing	En-route		Approach		Unconst. flight time	
					Planned dep.	Max delay		Max advance	Max delay	Max advance	Max delay	fr. IAF 1 to RWY	fr. IAF 2 to RWY
NLY966D	On-ground	A320	M	2	346	900	7846	60	300	0	1200	780	660
AFR007	Airborne	A388	H	1	NA	0	7920	60	300	0	1200	780	660
GW16Z	On-ground	A319	M	2	3451	900	7951	60	300	0	1200	780	660
AFR379	Airborne	B772	H	1	NA	0	8096	60	300	0	1200	780	660
AFR347	Airborne	A343	H	1	NA	0	8124	60	300	0	1200	780	660
GW198M	On-ground	A320	M	2	2086	900	8086	60	300	0	1200	780	660
DAL400	Airborne	A333	H	1	NA	0	8232	60	300	0	1200	780	660
UAL904	Airborne	B763	H	1	NA	0	8280	60	300	0	1200	780	660
DLH68H	On-ground	E190	M	2	2602	900	8302	60	300	0	1200	780	660
AFR639	Airborne	B77W	H	1	NA	0	8476	60	300	0	1200	780	660
DLH28W	On-ground	A321	M	2	3930	900	8430	60	300	0	1200	780	660
AAL786	Airborne	A333	H	1	NA	0	8544	60	300	0	1200	780	660
GW13J	On-ground	A319	M	2	2198	900	8498	60	300	0	1200	780	660
BEE5JA	On-ground	E170	M	1	3208	900	8608	60	300	0	1200	780	660
KLM11P	On-ground	B739	M	2	3758	900	8558	60	300	0	1200	780	660
AFR191	Airborne	A332	H	2	NA	0	8598	60	300	0	1200	780	660
BEE670U	On-ground	E190	M	1	3864	900	8664	60	300	0	1200	780	660
AAL62	Airborne	B763	H	1	NA	0	8732	60	300	0	1200	780	660
AFR135Q	On-ground	A319	M	2	1266	900	8766	60	300	0	1200	780	660
AFR1473	On-ground	E170	M	1	1740	900	8940	60	300	0	1200	780	660
AFR124C	Airborne	A321	M	2	NA	0	8886	60	300	0	1200	780	660
ACA880	Airborne	B77W	H	1	NA	0	8972	60	300	0	1200	780	660
LGL8011	On-ground	E145	M	2	5058	900	8958	60	300	0	1200	780	660
CSA3DZ	On-ground	A319	M	2	2398	900	8998	60	300	0	1200	780	660
AFR1747	Airborne	E170	M	2	NA	0	9082	60	300	0	1200	780	660
AFR341E	Airborne	A320	M	2	NA	0	9183	60	300	0	1200	780	660
AFR801F	On-ground	A320	M	1	4916	900	9416	60	300	0	1200	780	660
UAL987	Airborne	B763	H	1	NA	0	9512	60	300	0	1200	780	660
CSN347	Airborne	A332	H	2	NA	0	9583	60	300	0	1200	780	660
AFR1653	Airborne	A319	M	2	NA	0	9635	60	300	0	1200	780	660
COUNT	(16) Airborne (14) On-ground		(18) M (12) H	(14) IAF 1 (16) IAF 2									

**Table C.1**

Unit delay and advance cost (in euros per second), by flight phase, and by delay range (in minutes). Values based on estimations are in bold.

Aircraft type	At-gate				En-route				Approach				
	0 - 5	5 - 15	15 - 30	≥ 30	≤ 0	0 - 5	5 - 15	15 - 30	≥ 30	0 - 5	5 - 15	15 - 30	≥ 30
A319	0.23	0.62	1.29	3.18	-0.05	0.80	1.18	1.86	3.74	0.73	1.12	1.80	3.68
A320	0.27	0.7	1.47	3.63	-0.05	0.83	1.27	2.04	4.20	0.83	1.25	2.02	4.19
A321	0.33	0.8	1.76	4.36	-0.06	1.00	1.48	2.43	5.04	0.93	1.42	2.37	4.97
A332	0.6	1.35	2.84	7.18	-0.11	1.90	2.62	4.13	8.47	1.57	2.28	3.79	8.13
A333	0.6	1.38	2.94	7.41	-0.12	2.06	2.85	4.41	8.88	1.68	2.45	4.00	8.43
A343	0.66	1.53	3.27	8.25	-0.14	2.32	3.19	4.93	9.92	1.68	2.45	4.00	8.43
A388	0.99	2.26	4.86	12.34	-0.21	3.55	4.82	7.43	14.91	3.27	4.72	7.72	16.35
AT43	0.1	0.25	0.48	1.11	-0.01	0.23	0.37	0.60	1.23	0.23	0.37	0.60	1.22
AT72	0.13	0.33	0.64	1.54	-0.02	0.30	0.50	0.82	1.71	0.30	0.47	0.80	1.69
B733	0.23	0.6	1.24	3.04	-0.05	0.83	1.18	1.84	3.63	0.70	1.07	1.72	3.51
B734	0.27	0.67	1.4	3.44	-0.05	0.87	1.25	1.99	4.03	0.83	1.22	1.94	3.99
B735	0.23	0.53	1.12	2.71	-0.05	0.77	1.08	1.66	3.26	0.60	0.93	1.50	3.11
B738	0.3	0.75	1.56	3.84	-0.05	0.90	1.35	2.17	4.45	0.83	1.28	2.10	4.38
B739	0.3	0.72	1.52	3.76	-0.06	0.97	1.39	2.19	4.43	0.98	1.45	2.36	4.93
B744	0.8	1.88	4.03	10.24	-0.19	3.10	4.18	6.33	12.54	2.37	3.42	5.58	11.79
B752	0.33	0.87	1.86	4.63	-0.07	1.13	1.67	2.66	5.43	0.97	1.48	2.49	5.26
B763	0.57	1.22	2.56	6.43	-0.10	1.70	2.35	3.69	7.57	1.60	2.25	3.60	7.47
B772	0.62	1.44	3.07	7.73	-0.13	2.16	2.98	4.61	9.28	1.72	2.50	4.09	8.61
B77W	0.76	1.75	3.75	9.49	-0.16	2.69	3.68	5.68	11.43	2.11	3.06	5.00	10.56

(continued on next page)

**Table C.1** (continued).

Aircraft type	At-gate				En-route					Approach			
	0 – 5	5 – 15	15 – 30	≥ 30	≤ 0	0 – 5	5 – 15	15 – 30	≥ 30	0 – 5	5 – 15	15 – 30	≥ 30
DH8D	0.13	0.35	0.71	1.67	-0.02	0.37	0.57	0.92	1.89	0.37	0.57	0.92	1.89
E145	<b>0.11</b>	<b>0.28</b>	<b>0.57</b>	<b>1.32</b>	<b>-0.01</b>	<b>0.23</b>	<b>0.41</b>	<b>0.70</b>	<b>1.45</b>	<b>0.18</b>	<b>0.31</b>	<b>0.50</b>	<b>0.97</b>
E170	<b>0.18</b>	<b>0.44</b>	<b>0.92</b>	<b>2.21</b>	<b>-0.03</b>	<b>0.50</b>	<b>0.76</b>	<b>1.24</b>	<b>2.53</b>	<b>0.37</b>	<b>0.58</b>	<b>0.93</b>	<b>1.88</b>
E190	0.2	0.43	0.92	2.22	-0.04	0.60	0.87	1.34	2.64	0.60	0.85	1.32	2.62

**References**

Balakrishnan, Hamsa, Chandran, Bala G., 2010. Algorithms for scheduling runway operations under constrained position shifting. *Oper. Res.* 58 (6), 1650–1665. <http://dx.doi.org/10.1287/opre.1100.0869>.

Beasley, John E., Krishnamoorthy, Mohan, Sharaiha, Yazid M., Abramson, David, 2000. Scheduling aircraft landings: The static case. *Transp. Sci.* 34 (2), 180–197. <http://dx.doi.org/10.1287/trsc.34.2.180.12302>.

Bennell, Julia A., Mesgarpour, Mohammad, Potts, Chris N., 2011. Airport runway scheduling. *4OR* 9 (2), 115–138. <http://dx.doi.org/10.1007/s10288-011-0172-x>.

Birge, John R., Louveaux, François, 2011. *Introduction to Stochastic Programming*. Springer Science & Business Media.

Bolić, Tatjana, Castelli, Lorenzo, Corolli, Luca, Rignonat, Desirée, 2017. Reducing ATFM delays through strategic flight planning. *Transp. Res. E* 98, 42–59. <http://dx.doi.org/10.1016/j.tre.2016.12.001>.

Cook, Andrew J., Tanner, Graham, 2015. European airline delay cost reference values. Technical report, EUROCONTROL Performance Review Unit.

Corolli, Luca, Lulli, Guglielmo, Ntaimo, Lewis, Venkatachalam, Saravanan, 2015. A two-stage stochastic integer programming model for air traffic flow management. *IMA J. Manag. Math.* 28 (1), 19–40. <http://dx.doi.org/10.1093/imaman/dpv017>.

Dear, Roger G., 1976. The dynamic scheduling of aircraft in the near terminal area. Technical report R76-9, Massachusetts Institute of Technology. Flight Transportation Laboratory.

Frankovich, Michael J., 2012. Air traffic flow management at airports: A unified optimization approach. (Ph.D. thesis). Massachusetts Institute of Technology.

Fu, Michael C., et al., 2015. *Handbook of Simulation Optimization*. Vol. 216, Springer.

Hasevoets, Nathalie, Conroy, Paul, 2010. Arrival manager - implementation guidelines and lessons learned. Technical report, EUROCONTROL, URL <https://www.skybrary.aero/bookshelf/books/2416.pdf>.

Huo, Ying, Delahaye, Daniel, Sbihi, Mohammed, 2021. A probabilistic model based optimization for aircraft scheduling in terminal area under uncertainty. *Transp. Res. C* 132, 103374. <http://dx.doi.org/10.1016/j.trc.2021.103374>.

Ikli, Sana, Mancel, Catherine, Mongeau, Marcel, Olive, Xavier, Rachelson, Emmanuel, 2021. The aircraft runway scheduling problem: A survey. *Comput. Oper. Res.* 132, 105336. <http://dx.doi.org/10.1016/j.cor.2021.105336>.

Kaut, Michal, Wallace, Stein W., 2007. Evaluation of scenario-generation methods for stochastic programming. *Pac. J. Optim.* 3 (2), 257–271.

Keha, Ahmet B., de Farias, Ismael R., Nemhauser, George L., 2004. Models for representing piecewise linear cost functions. *Oper. Res. Lett.* 32 (1), 44–48. [http://dx.doi.org/10.1016/S0167-6377\(03\)00059-2](http://dx.doi.org/10.1016/S0167-6377(03)00059-2).

Khassiba, Ahmed, Bastin, Fabian, Cafieri, Sonia, Gendron, Bernard, Mongeau, Marcel, 2020. Two-stage stochastic mixed-integer programming with chance constraints for extended aircraft arrival management. *Transp. Sci.* 54 (4), 897–919. <http://dx.doi.org/10.1287/trsc.2020.0991>.

Khassiba, Ahmed, Bastin, Fabian, Gendron, Bernard, Cafieri, Sonia, Mongeau, Marcel, 2019. Extended aircraft arrival management under uncertainty: A computational study. *J. Air Transp.* 27 (3), 131–143. <http://dx.doi.org/10.2514/1.D0135>.

Kistan, Trevor, Gardi, Alessandro, Sabatini, Roberto, Ramasamy, Subramanian, Batuwangala, Eranga, 2017. An evolutionary outlook of air traffic flow management techniques. *Prog. Aerosp. Sci.* 88, 15–42. <http://dx.doi.org/10.1016/j.paerosci.2016.10.001>.

Lee, Hanbong, 2008. Tradeoff evaluation of scheduling algorithms for terminal-area air traffic control. (Master's thesis). Massachusetts Institute of Technology.

Liu, Ming, Liang, Bian, Zheng, Feifeng, Chu, Chengbin, Chu, Feng, 2018. A two-stage stochastic programming approach for aircraft landing problem. In: 15th International Conference on Service Systems and Service Management (ICSSSM). pp. 1–6. <http://dx.doi.org/10.1109/ICSSSM.2018.8465107>.

Meyn, Larry A., Erzberger, Heinz, 2005. Airport arrival capacity benefits due to improved scheduling accuracy. In: Proceedings of the 5th Aviation, Technology Integration and Operations and the 16th Lighter-than-Air Systems Technology and Balloon Systems Conferences. <http://dx.doi.org/10.2514/6.2005-7376>.

Psarafitis, Harilaos N., 1978. A dynamic programming approach to the aircraft sequencing problem. Technical report, Massachusetts Institute of Technology.

Samà, Marcella, D'Ariano, Andrea, D'Ariano, Paolo, Pacciarelli, Dario, 2014. Optimal aircraft scheduling and routing at a terminal control area during disturbances. *Transp. Res. C* 47, 61–85.

Scala, Paolo, Mota, Miguel Mujica, Wu, Cheng-Lung, Delahaye, Daniel, 2021. An optimization–simulation closed-loop feedback framework for modeling the airport capacity management problem under uncertainty. *Transp. Res. C* 124, 102937. <http://dx.doi.org/10.1016/j.trc.2020.102937>.

Shapiro, Alexander, Dentcheva, Darinka, Ruszczyński, Andrzej, 2021. *Lectures on Stochastic Programming: Modeling and Theory*, third ed. SIAM, Philadelphia, PA, USA.

Shone, Rob, Glazebrook, Kevin, Zografos, Konstantinos G., 2021. Applications of stochastic modeling in air traffic management: Methods, challenges and opportunities for solving air traffic problems under uncertainty. *European J. Oper. Res.* 292 (1), 1–26. <http://dx.doi.org/10.1016/j.ejor.2020.10.039>.

Sölveling, Gustaf, Clarke, John-Paul, 2014. Scheduling of airport runway operations using stochastic branch and bound methods. *Transp. Res. C* 45, 119–137. <http://dx.doi.org/10.1016/j.trc.2014.02.021>.

Sölveling, Gustaf, Solak, Senay, Clarke, John-Paul, Johnson, Ellis, 2011. Runway operations optimization in the presence of uncertainties. *J. Guid. Control Dyn.* 34 (5), 1373–1382. <http://dx.doi.org/10.2514/6.2010-9252>.

Tielrooij, Maarten, Borst, Clark, Van Paassen, Marinus M., Mulder, Max, 2015. Predicting arrival time uncertainty from actual flight information. In: Proceedings of the 11th USA/Europe Air Traffic Management Research and Development Seminar. FAA/EUROCONTROL, pp. 577–586.

Vié, Marie-Sklaerder, Zufferey, Nicolas, Leus, Roel, 2022. Aircraft landing planning under uncertain conditions. *J. Sched.* 1–26. <http://dx.doi.org/10.1007/s10951-022-00730-0>.

Zhu, Yongqiu, Goverde, Rob, 2020. Dynamic and robust timetable rescheduling for uncertain railway disruptions. *J. Rail Transp. Plan. Manage.* 15, 100196. <http://dx.doi.org/10.1016/j.jrtpm.2020.100196>.